



SAFER applications for water productivity assessments with aerial camera onboard a remotely piloted aircraft (RPA). A rainfed corn study in Northeast Brazil

Antônio Teixeira ^{a,*}, Edson Pacheco ^b, César Silva ^c, Marcia Dompieri ^d, Janice Leivas ^d

^a Water Resources Program (PRORH) from Federal University of Sergipe (UFS), Brazil

^b Embrapa Coastal Tablelands, Brazil

^c University of Campinas (UNICAMP), Brazil

^d Embrapa Territory, Brazil



ARTICLE INFO

Keywords:

Aerial images

Actual evapotranspiration

Biomass production

Zea mays L

ABSTRACT

Aerial images taken with a camera onboard a remotely piloted aircraft (ARP) at 4-cm resolution were used for rainfed corn water productivity (WP) assessments by applying the Simple Algorithm for Evapotranspiration Retrieving (SAFER) and the radiation use efficiency (RUE) Monteith's model in Northeast Brazil. We present a methodology based on the use of the visible and near infrared images from a Sequoia camera together with weather and actual yield data (Y_a), to model actual evapotranspiration (ET) and biomass production (BIO), retrieving water productivity based on both BIO (WP_{BIO}) and actual yield (WP_{Y_a}). Different nitrogen (N) fertilizing cover levels (0–250 kg ha⁻¹) and sources (nitrate – Nt and urea – Ur) were analyzed for supporting precision agriculture, aiming a fertilizing recommendation for good corn yield while reducing water use and N leaching problems. According to our statistical analyzes, there were no significant difference on ET values for the N treatments inside the analyzed phenological stages (PS) due to the proportional partition into soil evaporation and transpiration from seeding to harvest stages, but as BIO values is related to transpiration which in turn varied with PS until a certain limit, they affected WP till N cover fertilizing level of 150 kg ha⁻¹ for both Nt and Ur N sources. Regarding the growing season (GS) WP components, no significant differences were verified between Nt and Ur N sources, being the average values for ET, BIO, and Y_a , of 394 mm GS⁻¹, 17.3 t GS⁻¹, and 8.8 t GS⁻¹, which yielded mean WP_{BIO} and WP_{Y_a} of 4.4 kg m⁻³ and 2.2 kg m⁻³, corresponding to a harvest index (HI) around 0.50 considering all N cover fertilizing treatments. The most important finding of the current research is that the SAFER algorithm can be applied to estimate ET with high resolution aerial cameras without the thermal bands, and together with modelled BIO or Y_a data, WP assessments can be carried out following the principles of precision agriculture. The slightly lower WP values for Ur N source and the advantage of its lower both price and N leaching problems, Ur applications at 150 kg ha⁻¹ is recommended to save money while avoiding N leaching to the ground water, when compared with Nt source. For replication of the tested methods in other regions, simple calibrations of the modelling equations may be done with field or/and remote sensing measurements, to infer the specific environmental conditions.

1. Introduction

Effective crop fertilizing is one of the pathways to sustain precision agriculture with high yield levels while minimizing environmental problems, i.e. maximizing water productivity (WP). For WP assessments, it is important to make distinctions between the concepts of reference

(ET_0), actual (ET), and potential (ET_p) evapotranspiration. ET_0 is considered as the water flux from a grassed reference surface, with specific characteristics, while ET is the water flux involving all environmental conditions, while ET_p happens when the crop is under optimum root-zone moisture conditions (Allen et al., 1998). ET can be partitioned into transpiration and soil evaporation, and the magnitude

* Corresponding author.

E-mail addresses: heriberto@pq.cnpq.br, heriberto@academico.ufs.br, heribert@globomail.com (A. Teixeira), edson.patto@embrapa.br (E. Pacheco), cesaroliveira.f.silva@gmail.com (C. Silva), marcia.dompieri@embrapa.br (M. Dompieri), janice.leivas@embrapa.br (J. Leivas).

of these components depend on the root-zone moisture and crop stages (Fandiño et al., 2012; Consoli and Vanella, 2014; Rosa et al., 2016; Longo-Minnolo et al., 2020). The ratio ET/ET_0 , under optimum root-zone moisture conditions is known as the crop coefficient - K_c and can be used to estimate ET_p (Mateos et al., 2013; Venancio et al., 2021), while under non-optimum root-zone moisture conditions, this ratio can characterize crop water stress (Lu et al., 2011).

High WP levels in precision agriculture require maximizing farm inputs by using the best practices at good both spatial and temporal scales, but field measurements of relevant biophysical parameters through destructive sampling are time and cost intensive. Remote sensing methods offer rapid and cost-effective ways to support farmer decisions to optimize the WP components, offering a range of possibilities their assessments at suitable scales, when aiming to insure good yields minimizing negative environmental effects (Mulla, 2013; Marino et al., 2015; McShane et al., 2017; Campos et al., 2018; Silva et al., 2019; Teixeira et al., 2020a,b; Venancio et al., 2021).

In Northeast Brazil, one of the most important agricultural crops is corn (*Zea mays* L.), seeded at the start of the rainy season, under irrigation or rainfed conditions, for both human and animal feeding. According to Teixeira et al. (2014a,b), besides fertilizing managements, weather conditions drive ET and biomass production (BIO), and then the crop water productivity (WP), here considered as the ratio of BIO and actual yield (Y_a) to ET, being these biophysical indices also affected by the degree of the root-zone water stress (Ko and Piccini, 2009; Liu et al., 2010; Zhang et al., 2019; Nyolei et al., 2019).

Crop yield and plant responses to nitrogen (N) cover fertilizing varies significantly with the time of the year in response to root-zone moisture conditions (Bakhsh et al., 2000). Quantifying corn WP under different N cover fertilizing levels and sources is important for adaptations to climate and land-use changes, and mitigations of the negative effects of these changes. When biophysical parameters can be quantified by field measurements, site-specific knowledge can assist farmers for better water and crop managements. However, for in-depth monitoring of these parameters during each phenological stage (PS), high spatial resolution remote sensing data taken with aerial cameras without influence of cloudiness are more suitable, when aiming to meet the principles of precision agriculture (Tunca et al., 2018; Manfreda et al., 2018; Maes and Steppe, 2019).

In the current paper, WP assessments were done during four rainfed corn crop PS and for the growing season (GS) in the Sergipe state, Northeast Brazil. Under water scarcity conditions in this region, one of the biggest challenges for optimizing crop and water managements is through WP improvements. For good corn yields, N cover fertilizing is needed in expressive amounts being this nutrient highlighted as the most dynamic one in the plant root-zones. Nitrate (Nt) and Urea (Ur) are common N sources used for N cover fertilizing, however, besides being more expensive, Nt cause more environmental problems because of high N leaching rates to the ground water when comparing to Ur (Pacheco et al., 2018). The physical and chemical properties of the soil, as well as root-zone moisture status, will affect N dynamics. Thus, crop management systems for optimizing N cover fertilizing are important to increase corn WP (Colaço and Bramley, 2018).

Currently, precision agriculture research using remotely sensed data can help N fertilizing strategies (Sharma and Bali, 2018; Colaço and Bramley, 2018), plant protection managements (Mahlein et al., 2012; Sedina et al., 2017), biomass estimations (Teixeira et al., 2019; Togéiro de Alckmin et al., 2020); and to retrieve physical (Ballabio et al., 2016), biological (Yigini and Panagos, 2016), and chemical (Ballabio et al., 2019) properties of soils. However, there are still lacks of remote sensing studies for corn WP modelling at the level of precision agriculture in Brazil, with few ones done at irrigation pivot parcels with Landsat 8 images at spatial resolutions ranging from 30 to 120 m (Teixeira et al., 2014b; Venancio et al., 2021).

Remote sensing algorithms to quantify the WP components have been developed, presenting advantages and shortcomings among them.

The Penman-Monteith (PM) equation has been suggested by applying remotely sensed vegetation indices, together with agrometeorological data (Nagler et al., 2013; Senay et al., 2017; Vanino et al., 2018). The PM equation is also used in the well-known METRIC - Mapping Evapotranspiration with High Resolution and Internalized Calibration algorithm (Allen et al., 2007), which has the advantage of up scaling the instantaneous ET value to daily timescale. The SAFER algorithm, based on the PM equation, was developed (Teixeira, 2010) and validated for its application with and without the thermal spectral radiances in several agroecosystems of Northeast Brazil (Araujo et al., 2019; Silva et al., 2019; Teixeira et al., 2020a,b; Venancio et al., 2021).

Considering the operability and no requirements of thermal bands the SAFER algorithm was chosen for the current research. Even that the algorithm has been successfully applied for corn WP determinations, by coupling satellite images and weather data, for both rainfed (Teixeira et al., 2014a) and irrigation Brazilian conditions (Teixeira et al., 2014b; Venancio et al., 2021), the development of aerial cameras to be used onboard remotely piloted aircrafts (RPA) without cloud cover interference demand tests for applications with high resolution images to subsidize precision agriculture (Gago et al., 2015; Pádua et al., 2017). This issue increases in importance, when aiming water and crop managements under the actual water scarcity conditions experienced by several agroecosystems.

The objective of the current research was to test the application of the SAFER algorithm coupled with the Monteith's radiation use efficiency (RUE) model (Monteith, 1977), to assess the WP components by using the visible and infrared bands of aerial images onboard at a RPA, in rainfed corn crop in Northeast Brazil, analyzing the effects of different N cover fertilizing levels and sources in the magnitude of these components. The results are useful for recommendation of N fertilizing management when aiming to improve WP under water scarcity conditions. With the success of the tests with the corn reference crop, the models can be used in other regions and crops applying simple corrections for calibration coefficients of the modelling equations to infer specific environmental conditions.

2. Materials and methods

2.1. Characteristics of the study area, phenological stages and fertilizing management

Fig. 1 shows the location of the experimental area with corn plots cover fertilized under different nitrogen (N) levels and sources, in the municipality of Nossa Senhora das Dores, Sergipe state, Northeast Brazil.

The experimental area, latitude $10^{\circ}27'44''$ S, longitude $37^{\circ}11'38''$ W, and altitude of 200 m, is in a region ranging from sub-humid to dry climates, with a mean annual air temperature (T_a) of 24.6°C , and total precipitation (P) of 1150 mm yr^{-1} , being rainfalls concentrated from March to August. The natural ecosystems may be considered as a transition between coastal tablelands and semi-arid, however the natural species are being replaced by rainfed and irrigated crops in several areas. The soil is classified as red-yellow clay with clayish texture, dystrophic, and wavy relief. **Table 1** presents the chemical and physical properties of the soil at 0.00–0.20 m depth according to Pacheco et al. (2018).

According to **Table 1**, the soil is characterized by a poor fertility for corn crop. The value for potential of hydrogen (pH) together with high sum of aluminum (Al) and hydrogen (H), representing 47% of the Exchange Capacity of Cations (ECC) defined an average acidity condition, what required application of 1.2 t ha^{-1} of dolomitic limestone before corn seeding. The low contents of organic matter (OM), phosphorus (P), and potassium (K) required the foundation fertilizing of NPK at the proportion of $40\text{--}100\text{--}80 (\text{kg ha}^{-1})$, for all plots. Besides correcting the acidity conditions, the dolomitic limestones also increased the levels Calcium (Ca) and Magnesium (Mg), previously representing only 32% and 19% of the ECC. According to the clay content, the soil presents

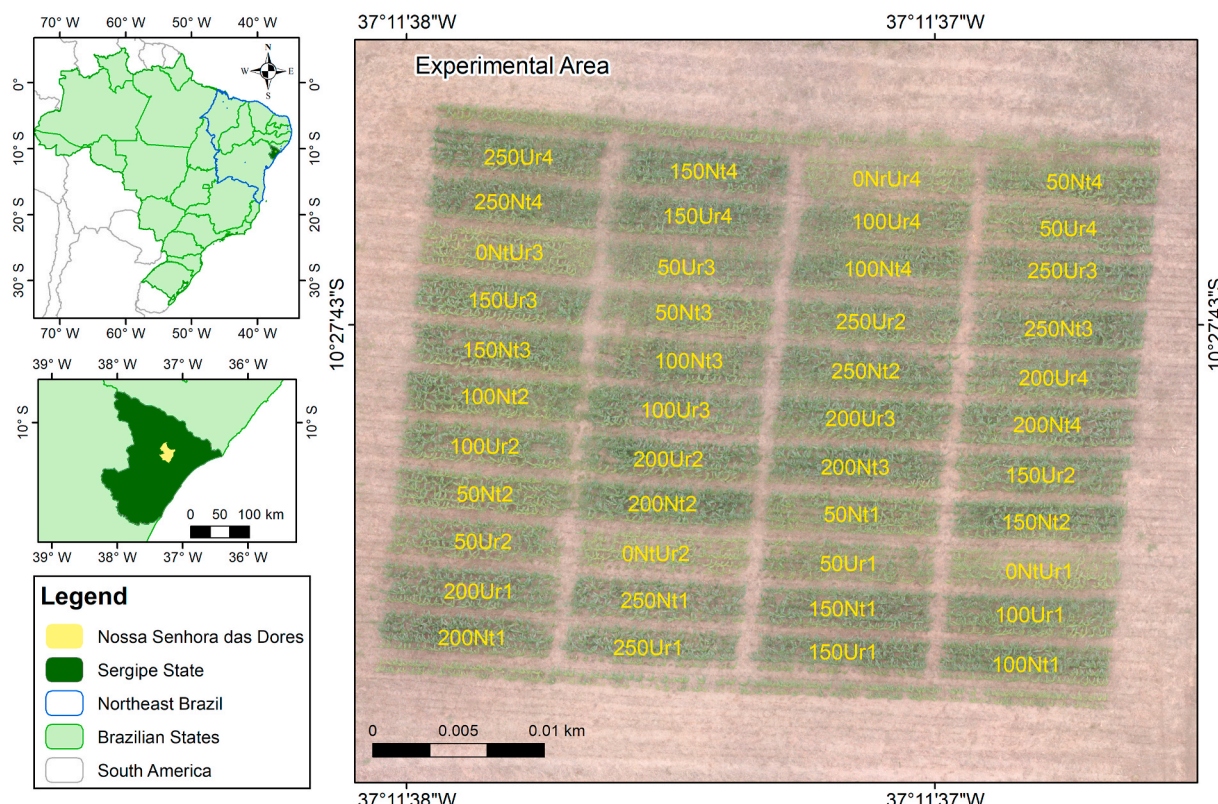


Fig. 1. Location of the experimental area, corn plots cover fertilized with different nitrogen (N) levels from nitrate – Nt (27% of N) and urea – Ur (46% of N) sources, at 0, 50, 100, 150, 200 e 250 kg ha⁻¹, in the municipality of Nossa Senhora das Dores, Sergipe state, Northeast Brazil.

Table 1

Chemical and physical properties for the soil at depths from 0.00 to 0.20 m for the experimental area, in the municipality of Nossa Senhora das Dores, Sergipe state, Northeast Brazil.

| pH (-) | OM (dag kg ⁻¹) | P (mg dm ⁻³) | K (cmole dm ⁻³) | Ca (cmole dm ⁻³) |
|------------------------------|------------------------------|----------------------------------|-------------------------------|---------------------------------|
| 5.49 | 2.34 | 6.35 | 65.33 | 2.10 |
| Mg (cmole dm ⁻³) | Al (cmole dm ⁻³) | H + Al (cmole dm ⁻³) | ECC (cmole dm ⁻³) | Clay Content g kg ⁻¹ |
| 1.25 | <0.10 | 3.13 | 6.65 | 290 |

*pH – potential of hydrogen in water; OM – Organic matter; ECC – Exchange Capacity of Cations.

good drainage conditions.

The general corn seeding time is from the second half of May to the first half of June, with harvest occurring from the second half of October to the first half of November, depending on the cultivar (Pacheco et al., 2018). Following Fancelli and Dourado Neto (2000) the corn phenological stages (PS) considered in the current research are described in Table 2.

The experimental design was of randomly blocks with four repetitions, in a factorial scheme 5 (N cover levels) x 2 (N cover sources), and a witness (0 N cover fertilizing). Sowing (S) time was in Jun 06, 2017, over 10-m six-lines plots, with the plants spaced 0.50 m between lines of the Syngenta cultivar, totaling 44 experimental plots of 30 m², in a corn cropped area of 1320 m² (see Fig. 1). Regarding the experimental treatments, it was considered six N cover fertilizing levels: 0, 50, 100, 150, 200, and 250 kg ha⁻¹, via nitrate (Nt) – 27% of N and urea (Ur) – 46% of N, when the corn plants presented four leaves (June 22, 2017), at the V4 vegetative PS (see Table 2).

The effect of the cover fertilizing under different N levels and sources on water productivity (WP) dynamics in terms of BIO were assessed for

the RPA flights at V6, V10, PF, and FF stages. The harvest was done with a mechanical harvester, by weighting the grains in an automatic balance and with up-scaling techniques, it was also possible to quantify WP in terms of both BIO and actual yield (Y_a) at the growing season (GS) timescale. The average values and standard deviations (SD) of the WP components involving 6000 pixels, at a 4-cm spatial resolution, in the center of the plots for each N treatment were considered during the analyzed PS and for GS.

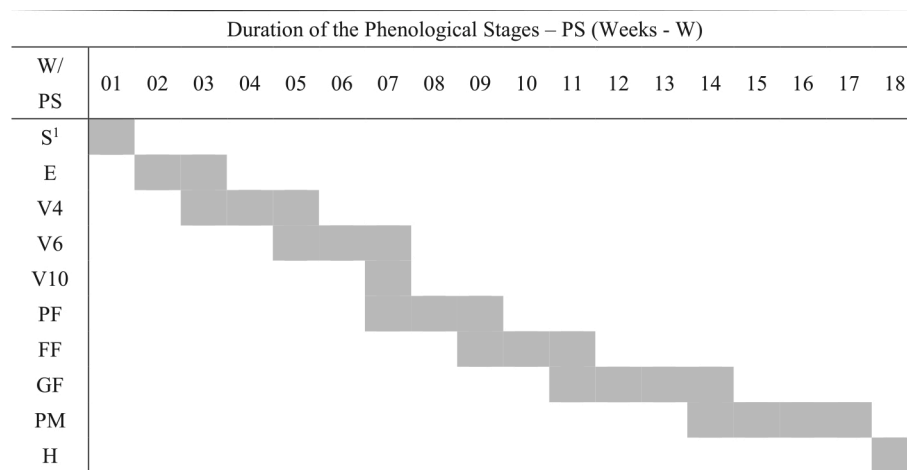
2.2. Agrometeorological and remote sensing data processing

One agrometeorological station was installed at 300 m from the experimental area and the weather data used together with remote sensing parameters for modelling the WP components. The weather data were daily values of incident global solar radiation – R_G; air temperature – T_a (maximum, mean, and minimum values) and relative humidity – RH; and wind speed at a height of 2 m – u₂, inputted for the reference evapotranspiration (ET₀) calculations by the Penman-Monteith method (Allen et al., 1998). However, besides being used for ET₀ calculations, R_G and mean T_a were also input data for the radiation balance components, which together surface albedo – α₀ and the Normalized Difference Vegetation Index – NDVI, allowed the surface temperature (T₀) estimations at daily timescale (Leivas et al., 2017; Araujo et al., 2019; Silva et al., 2019; Teixeira et al., 2020a,b). The agrometeorological station was programmed to collect data at each minute and storage half-hour averages and then 24-h mean values were considered for the SAFER and RUE coupled applications.

The aerial images were taken at around local time of 13 UTC (GMT-3) in July 11 (PS V6), July 21 (PS V10), August 04 (PS PF), and August 11 (PS FF) of 2017, with a multispectral camera Parrot Sequoia-Mica Sense, onboard a remotely piloted aircraft (RPA), Tarot 650 Iron Man, navigator “Pixhawk”, by using an interface software “Mission Planner”. The mosaic building software was the Agisoft Photoscan (version 1.6.6,

Table 2

Phenological stages (PS) for the rainfed corn crop, in the municipality of Nossa Senhora das Dores, Sergipe state, Northeast Brazil.



¹S – Sowing; E – Emergency; V4, V6, and V10 – Vegetative stages with four, six, and ten leaves, respectively; PF – Pre-flowering; FF – Full flowering; GF – Grain filling; PM- Physiological maturation; H – Harvest.

<http://www.agisoft.com/downloads/installer/>), considering longitudinal and lateral overlaps of 80% and 60%, respectively.

Table 3 shows the specifications of the multispectral camera Parrot Sequoia-Mica Sense.

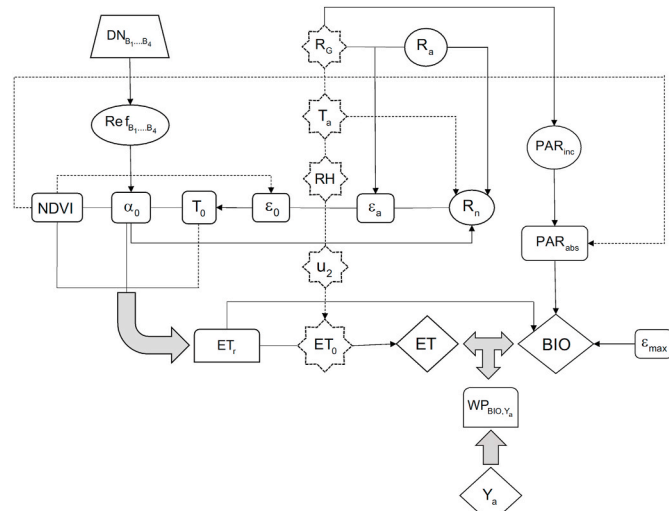
With the flights at a 40-m height, the images were at a 4-cm spatial resolution. The total RPA overflowed area was 1.8 ha, covering the studied corn crop, natural vegetation, and bare soil from which the corn plots were cut for WP assessments. For calibrations of the remote sensing parameters from Sequoia (Sq) measurements, reflectance values from Landsat 8 (L8) images (bands 1 to 7, spatial resolution of 30 m), for the days June 28, July 14, July 30, August 15, and August 31 of 2017, orbital/pointer 215/067, were used considering the total RPA overflowed area. In this area covering mixed surface types, one L8 pixel involved an average for 750 Sq pixel values. The modelling equations for Landsat had been previously calibrated with field energy balance experiments involving hydrological contrasting vegetation types in Northeast Brazil (Teixeira, 2010).

Fig. 2 presents the flowchart for the corn WP modelling by applying the SAFER algorithm and the RUE model starting from the Sq digital numbers from bands 1 to 4 (DN_{B_1} , DN_{B_2} , DN_{B_3} , and DN_{B_4}).

Note: $DN_{B_1 \dots B_4}$ - Digital numbers from bands 1 to 4; $Ref_{B_1 \dots B_4}$ - Reflectance values from bands 1 to 4; α_0 - Surface albedo; NDVI - Normalized Difference Vegetation Index; T_0 - Surface temperature; R_g - Incident global solar radiation; R_a - Top-atmosphere radiation; T_a - Air temperature; RH - Relative humidity; u_2 - Wind speed at a height of 2 m; ET_r - Ratio of actual to reference evapotranspiration; ET - Actual evapotranspiration; ET_0 - Reference evapotranspiration; ϵ_0 - Surface emissivity; ϵ_a - Atmospheric emissivity; R_n - Net radiation; PAR_{inc} - Incident photosynthetically active radiation; PAR_{abs} - Absorbed

Table 3
Specifications of the multispectral camera Parrot Sequoia-Mica Sense.

| Band | Bands/Image Characteristics | | | | |
|----------------------------|-----------------------------|-----------------|-------------------|---------------------|-------------------|
| | Centre Wavelength (nm) | Band Width (nm) | Focal Length (mm) | Image Size (pixels) | Field of View |
| Green (B ₁) | 550 | 40 | 3.98 | 1280 × 960 | Horizontal: 61.9° |
| Red (B ₂) | 660 | 40 | | | Vertical: 48.5° |
| Red Edge (B ₃) | 735 | 10 | | | Diagonal: 73.7° |
| NIR (B ₄) | 790 | 40 | | | |



one Landsat DN pixel value represents an average of 750 Sq DN pixel values for hydrologically contrasting surfaces.

To obtain the regression coefficients of Eq. (1), the L8 Ref values from bands B₁ to B₇ for the total RPA overflowed area were downloaded from the United States Geological Survey (USGS) site (<https://earthexplorer.usgs.gov/>), and the weights for each band applied to the L8 albedo values (α_{0_L8}) according to Teixeira et al. (2019). Although the L8 images being acquired at different days regarding the Sq image dates, the α_{0_L8} relation with the accumulated degree-days (DD_{ac}), allowed to obtain the Sq α_0 counterpart values for the RPA flight days.

Corn crop DD_{ac}, from sowing (S) to harvest (H) stages, were calculated considering a basal temperature of 10 °C, according to Teixeira et al. (2014b).

$$DD_{ac} = \sum_s^H (T_a - 10) \quad (2)$$

where T_a is the mean air temperature.

The α_{0_L8} values for the four RPA flight dates were estimated by the relation depicted in Fig. 3a and the regression coefficients of Eq. (1) obtained (Fig. 3b):

It is emphasized that if one has already the band reflectance values available from the RPA onboard camera, through control ground targets, the weights for α_0 calculations may be directly applied to Ref values (Teixeira et al., 2019). On the other hand, the coefficients from Eq. (1) can be recalibrated with field measurements of incident and reflected solar radiation for specific hydrologically contrasting areas.

The Normalized Difference Vegetation Index (NDVI) was calculated from the digital numbers of NIR (DN_{B4}) and RED (DN_{B2}) Sq bands:

$$NDVI = \frac{DN_{B4} - DN_{B2}}{DN_{B4} + DN_{B2}} \quad (3)$$

As the Sq camera does not have a thermal band, T₀ was retrieved by the residual method, applying the Stefan-Boltzmann equation to estimate the long-wave radiation components (Ramírez-Cuesta et al., 2018):

$$T_0 = \sqrt[4]{\frac{R_G(1 - \alpha_0) + \sigma \epsilon_a T_a^4 - R_n}{\sigma \epsilon_0}} \quad (4)$$

where R_G is the incident global solar radiation; ϵ_a is the surface emissivity, R_n is the net radiation, σ is the Stefan-Boltzmann constant (5.67 × 10⁻⁸ W m⁻² K⁻⁴), and ϵ_0 is the surface emissivity.

The residual method to estimate T₀ has been successfully tested in distinct Brazilian agroecosystems (Teixeira et al., 2019, 2020a,b; Araujo et al., 2019; Silva et al., 2019; Rampazo et al., 2020). The suitability of retrieving the WP components, without the satellite thermal bands, has been also demonstrated in other recent studies around the world (Castelli et al., 2018; Rozenstein et al., 2018; Vanino et al., 2018; Mokhtari et al., 2019; Longo-Minnolo et al., 2020). In this way, it is possible to capture

the water stress effects without the need of the thermal portion of the electromagnetic spectrum (Consoli and Vanella, 2014).

The ϵ_a term from Eq. (4) was acquired as a function of the short-wave atmospheric transmissivity (τ_{sw}), which in turn was taken as the ratio of R_G to the solar radiation at the top of the atmosphere (R_a).

$$\epsilon_a = a_A (\ln \tau_{sw})^{b_A} \quad (5)$$

with a_A and b_A being the regression coefficients, a_A = 0.94 and b_A = 0.10, resulted from field radiation balance measurements in a range of contrasting environmental conditions over irrigated crops and natural vegetation in Northeast Brazil (Teixeira, 2010).

The daily R_n values were estimated throughout the Slob equation (Teixeira et al., 2020a,b):

$$R_n = (1 - \alpha_0)R_G - a_L \tau_{sw} \quad (6)$$

with the regression coefficient a_L determined through its relationship with T_a.

The surface emissivity (ϵ_0) was estimated according to Silva et al. (2019), Araujo et al. (2019), and Santos et al. (2020):

$$\epsilon_0 = a_0 \ln(NDVI) + b_0 \quad (7)$$

where a₀ and b₀ being the regression coefficients, a₀ = 0.06 and a₀ = 1.00, resulted from field measurements of the emitted surface radiation and T₀, together with remote sensing calculations of NDVI in Northeast Brazil (Teixeira, 2010).

The evapotranspiration ratio (ET_r = ET/ET₀), was estimated from the remote sensing parameters (Dehziari and Sanaienejad, 2019; Santos et al., 2020; Venancio et al. (2021):

$$ET_r = \exp \left[a_{sf} + b_{sf} \left(\frac{T_0}{\alpha_0 NDVI} \right) \right] \quad (8)$$

where a_{sf} and b_{sf} are regression coefficients, respectively 1.8 and -0.008, for the semi-arid conditions of Northeast Brazil, resulted from simultaneous field and Landsat measurements of ET and ET₀, together with α_0 , T₀, and NDVI, respectively (Teixeira, 2010). However, in the current paper, these regression coefficients were calibrated considered the ET_{r,L8} values as reference.

To calibrate the a_{sf} and b_{sf} regression coefficients from Eq. (8), ET_r values from L8 images were also related to DD_{ac} (Fig. 4a), and the estimated ET_{r,L8} values for the RPA flight dates were related to α_0 , NDVI, and T₀ (°C) values from Sq camera measurements (Fig. 4b):

The images covered the total RPA overflowed area, including the studied corn crop, natural vegetation, and bare soil, meaning that one Landsat ET_r pixel value involved an average of 750 Sq α_0 , NDVI, and T₀ pixel values. The calibrated regression coefficients a_{sf} and b_{sf} of 1.6 and -0.007 were then used in Eq. (8) and the daily ET₀ values (Allen et al., 1998) multiplied by the ET_r Sq pixel values, giving the corn daily ET

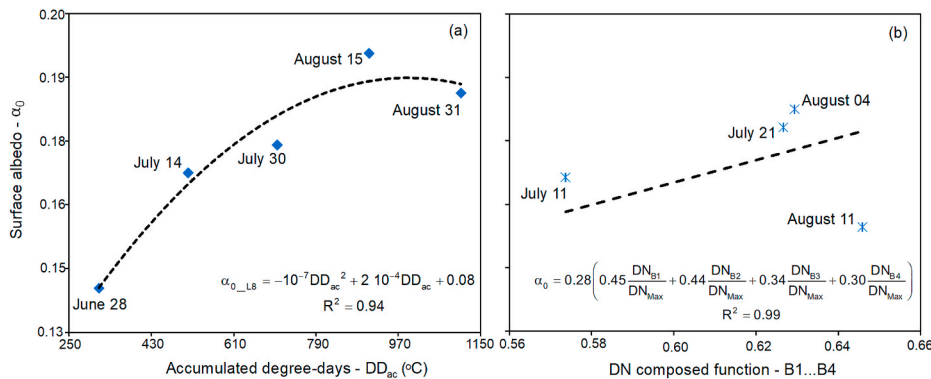


Fig. 3. Relationships between the Landsat 8 (L8) surface albedo values (α_{0_L8}) and the corn accumulated degree-days - DD_{ac} (a); and between α_{0_L8} with DN measurements from Sequoia (Sq) camera (b).

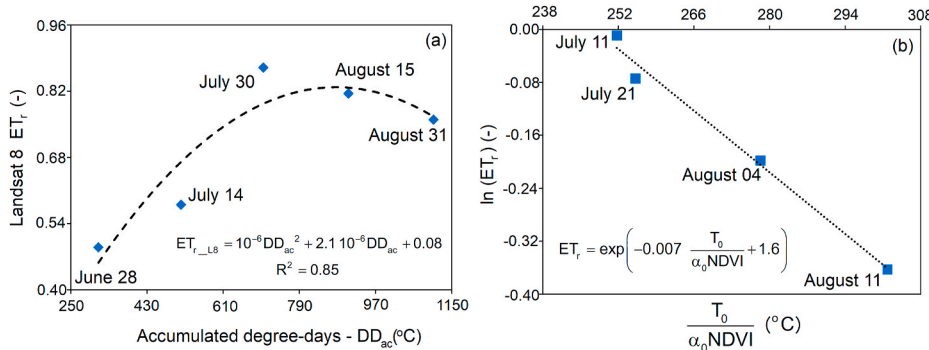


Fig. 4. Relationships between the Landsat 8 (L8) ratio of actual - ET to reference - ET₀ evapotranspiration (ET_r_{L8}) values and the corn accumulated degree-days - DD_{ac} (a); and between the estimated ET_r_{L8} and the remote sensing parameters surface albedo - α_0 , Normalized Difference Vegetation Index – NDVI, and surface temperature – T₀ (°C) acquired with the Sequoia (Sq) camera for the Remotely Piloted Aircraft (RPA) flight dates.

rates:

$$ET = ET_r ET_0 \quad (9)$$

The incident photosynthetically active radiation (PAR_{inc}) was estimated by:

$$PAR_{inc} = a_p R_G \quad (10)$$

where a_p is a regression coefficient found to be 0.44 for the Northeast Brazil (Teixeira et al., 2019).

The absorbed PAR (PAR_{abs}) was calculated as:

$$PAR_{abs} = f_p PAR \quad (11)$$

being the fraction of the absorbed PAR (f_p) estimated from NDVI:

$$f_p = a_p NDVI + b_p \quad (12)$$

where a_p and b_p are regression coefficients which in previous study for mixed agroecosystems were estimated respectively as 1.26 and -0.16 (Bastiaanssen and Ali, 2003).

The respective a_p and b_p original coefficients of 1.26 and -0.16 have been successfully validated with L8 images in some Brazilian Northeast agroecosystems (Araujo et al., 2019; Teixeira et al., 2019, 2020a), and by using them with the L8 images, the relation between PAR_{abs} and corn DD_{ac} values were used for Sq calibrations considering the Sq NDVI values for the RPA flight dates:

The images covered the total RPA overflowed area, including the studied corn crop, natural vegetation, and bare soil, meaning that one Landsat f_p pixel value involved an average of 750 Sq NDVI pixel values. The coefficients a_p (1.29) and b_p (-0.10) from Fig. 5b were used in Eq. (12) for BIO estimations, introducing the root-zone moisture effect through ET_r (Araujo et al., 2019; Teixeira et al., 2019, 2020a,b):

$$BIO = \sum (\varepsilon_{max} ET_r PAR_{abs} 0.864) \quad (13)$$

where ε_{max} is the maximum radiation efficiency use, considered as 2.45 MJ g MJ⁻¹ for corn crop (Teixeira et al., 2014a), and 0.864 is the unit conversion factor.

Having Y_a data available, and up scaling both ET_r and f_p for the corn GS, WP at this timescale was assessed based on both, BIO and Y_a:

$$WP_{BIO,Y_a} = \frac{BIO \text{ or } Y_a}{ET} \quad (14)$$

To upscale ET_r, its relationship with GD_{ac} for Sq measurements was used for each N cover fertilizing treatment considering the sowing (S) and harvest (H) time value of 0.30 and 0.50, respectively, for all N cover fertilizing treatments (Allen et al., 1998; Teixeira et al., 2014b). For f_p, the relationship below was applied to GS ET_r averages and used together with the R_G and ET₀ average GS data. According to Mateos et al. (2013), interpolated vegetation indices are subject to less uncertainty than interpolated ET values.

$$f_p = a_{pr} ET_r + b_{pr} \quad (15)$$

where the regression coefficients a_{pr} and b_{pr} were 0.60 and 0.30, with a R² around 0.80.

For some water productivity (WP) components, differences between the average pixel values among N cover treatments were not clear, therefore a more robust statistical tool was used to assess these differences. Analyses of variance (ANOVA) were performed using 2-way ANOVA in R (ver. 3.5.1) with a pairwise comparison by applying the Tukey honestly significant difference (HSD) post-hoc test, to assess their differences at 5% significance level, regarding the two N sources (nitrate- Nt and urea - Ur), the six N levels (0, 50, 100, 150, 200, and 250 kg ha⁻¹), and the four analyzed phenological stages - PS (V6, V10, PF,

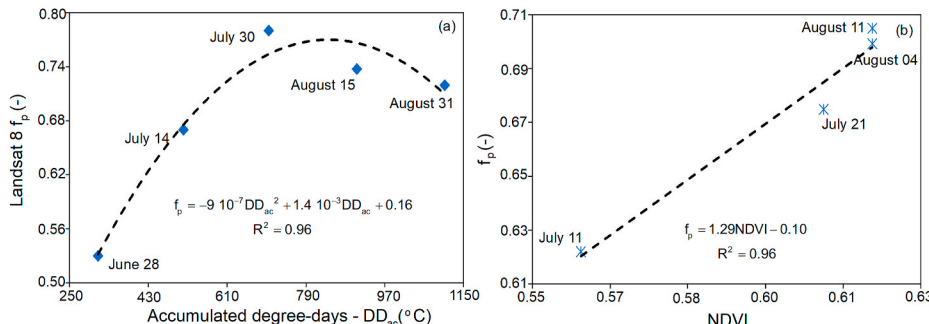


Fig. 5. Relationships between the fraction of absorbed photosynthetically active radiation fraction (f_p) from Landsat 8 (L8) measurements and the corn accumulated degree-days (DD_{ac}) (a); and the L8 estimated f_p with the Normalized Difference Vegetation Index (NDVI) from Sequoia (Sq) measurements for the Remotely Piloted Aircraft (RPA) flight dates.

and FF).

Before each ANOVA test the data were previously analyzed to confirm that it matched the basic assumptions: a) the responses for each N cover treatment presented normal population distributions with the very high spatial resolution; b) the normal distributions presented similar variances in statistically terms (for this reason the standard deviations are shown in all tables), and c) the data are independent, as that the samples were taken randomly). HSD is an integral part of ANOVA to test the equality of at least three group means. Statistically significant results indicate that not all the group means are equal, exploring differences between them while controlling the experiment-wise error rate.

3. Results and discussion

3.1. Weather conditions

As the corn WP components depend on the root-zone moisture conditions, which in turn are related to rainfall amounts and atmospheric demands, the weather parameters related to the climatic water balance were firstly analyzed. Fig. 6 presents the daily values, during the year 2017, for totals of precipitation (P) and reference evapotranspiration (ET_0); and for the averages of daily global solar radiation (R_G) and air temperature (T_a), in terms of Day of the Year (DOY).

From Fig. 6a, rainfalls were concentrated from the end of April (DOY 118) to September (DOY 267), with top P values above 10 mm d^{-1} , however, occurring week periods without rains. The annual P of 1153 mm yr^{-1} coincided with the long-term value for the study region

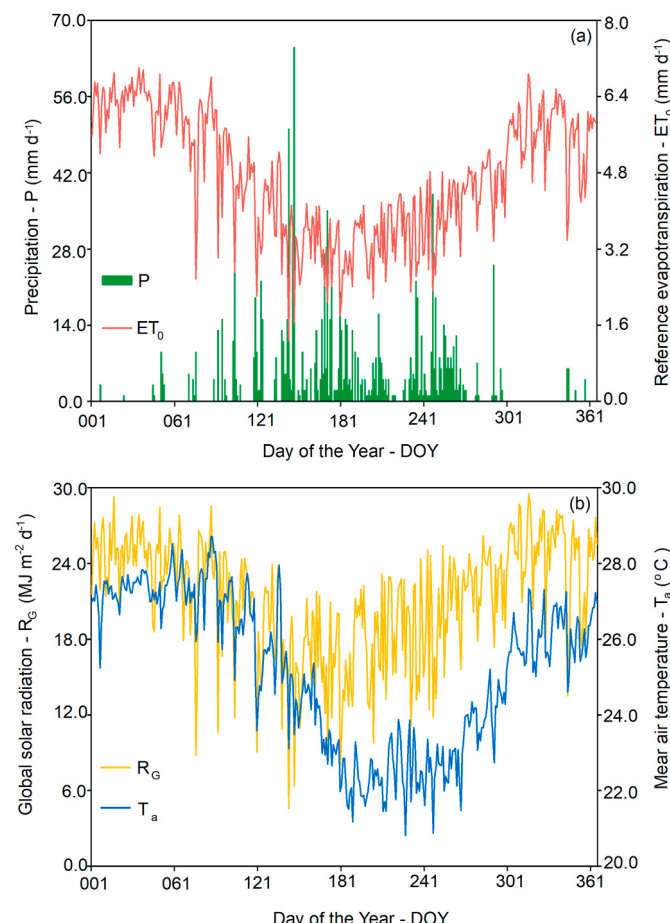


Fig. 6. Daily totals for precipitation (P) and reference evapotranspiration (ET_0); and daily mean values for global solar radiation (R_G) and air temperature (T_a), according to the Day of the Year (DOY), during 2017 in the municipality of Nossa Senhora das Dores, Sergipe (SE) state, Northeast Brazil.

reported in Pacheco et al. (2018). Considering the atmospheric demands, ET_0 values higher than 5.0 mm d^{-1} happened at the beginning of the year (from January to the first half of April, DOY 001 to 102), and during the last quarter of the year (from the end of October to December, DOY 301 to 365).

The R_G and T_a tendencies followed those for ET_0 , with respective mean daily values above $24.0 \text{ MJ m}^{-2} \text{ d}^{-1}$ and $26.0 \text{ }^\circ\text{C}$ in the beginning and in the end of the year; while the corresponding lowest ones, below $18.0 \text{ MJ m}^{-2} \text{ d}^{-1}$ and $22.0 \text{ }^\circ\text{C}$ occurred in the middle of the year (Fig. 6b).

Thus, the best corn root-zone moisture conditions happened in the middle of the year, but under the lowest atmospheric demands, which limited somewhat both ET and BIO rates, even under good rainfall-water availability.

3.2. Actual evapotranspiration

Fig. 7 shows the spatial distribution, average pixel values, and standard deviations (SD), for the daily rates of corn actual evapotranspiration (ET), considering the four analyzed phenological stages (PS), during the year 2017.

According to Fig. 7, there was a strong increase on ET rates along the four analyzed PS for all N cover fertilizing levels and sources, with mean pixel values ranging from $2.17 \text{ to } 4.44 \text{ mm d}^{-1}$ and standard deviations (SD) representing 59% and 33% of the averages, for the V6 (July 11, DOY 192) and PF (August 04, DOY 202) stages, respectively. However, besides PS, the average and SD values are also related to corn root-zone moisture, which in turn depend on the climatic water balance. Considering the ET_r pixel values (Eq. (8)) as a root-zone moisture indicator, with ET_0 from Fig. 6a, and the mean ET values from Fig. 7 for the V6, V10, FF, and FF, respectively, this indicator ranged from 0.59 (V6) to 1.03 (FF).

To assess the ET rates for each of the eleven N treatments (Nt and Ur sources at $0-250 \text{ kg ha}^{-1}$ N levels, with four repetitions) in each of the four analyzed PS, the centers of the individual corn plots were cut (see also the right side of Fig. 1), and the averages and SD values for around 6000 pixels in each plot considered.

Table 4 presents ET average and SD values, considering the N cover fertilizing levels and sources for each of the N treatment, together with the results of the pairwise comparison by group, using the Tukey HSD post-hoc test performed for each PS, while Table 5 shows detailed results of the ANOVA test for ET.

As the ET pixel values represented by the images in Fig. 7 depended on the root-zone moisture levels, which in turn are related to the climatic water balance involving previous and actual conditions, the following analyses considered the magnitudes of P and ET_0 ten days before the image acquisitions, with weather data depicted in Fig. 6a.

In the V6 stage (July 11, DOY 192), with ET pixel average values lower than 2.00 mm d^{-1} , the highest rates were for N cover fertilizing treatment 200NtUr, 20% above of those from the control one (0NrUr). For all corn plots, ET for the Ur source was only 8% higher than those for the Nt one. The previous 10-day P and ET_0 values were respectively, 66.0 and 30.0 mm , resulting in a climatic water excess ($P - ET_0 > 0$) of 36.0 mm . Thus, all treatments were well rainfall-water supplied in this PS, with ET_r values above 0.52 for both N cover fertilizing sources at low soil cover, but averaging 0.56 and 0.60 for Nt and Ur, respectively.

During the V10 stage (July 21, DOY 202), the plots with N cover applications at 100 kg ha^{-1} from Nt (100Nt) and 200 kg ha^{-1} from Ur (200Ur), presented the highest ET rates, above 7% of those for 0NrUr, but lower than 3.00 mm d^{-1} . Considering all corn plots, ET rates for Ur were only 2% higher than those for Nt. The previous 10-day P and ET_0 values (Fig. 6a) were respectively of 23.0 and 34.0 mm , resulting in a climatic water deficit ($P - ET_0 < 0$) of 11.0 mm . However, the ET_r values were above 0.94 for both N cover fertilizing sources, but averaging 0.97 and 0.99 for Nt and Ur, respectively, indicating good water storage in the root-zone from the previous rainier period, at increasing soil cover

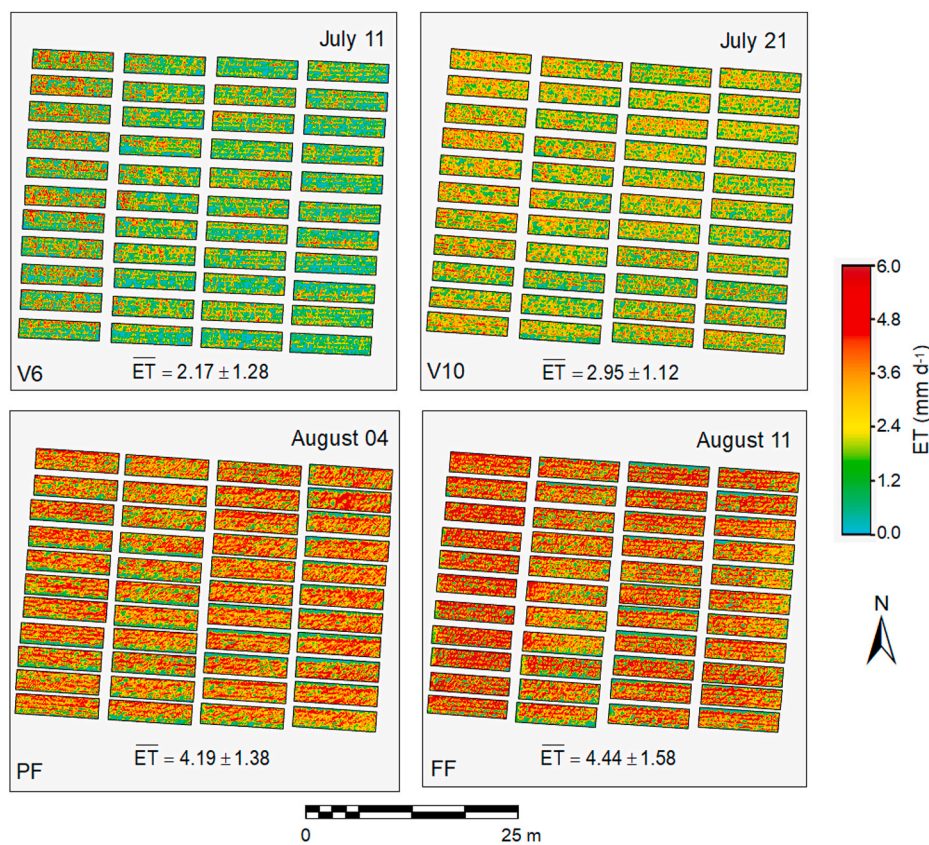


Fig. 7. Spatial distribution, average pixel values, and standard deviations (SD), for the daily corn actual evapotranspiration (ET), during four analyzed phenological stages (PS) in 2017. V6 – Vegetative stage with six leaves per plant (July 11, DOY 192), V10 – vegetative stage with ten leaves per plant (July 21, DOY 202), PF – reproductive stage pre flowering (August 04, DOY 216), and reproductive stage FF - full flowering (August 11, DOY 223).

Table 4

Average pixel values and standard deviations (SD) of actual evapotranspiration (ET), considering the N cover fertilizing levels ($0\text{--}250 \text{ kg ha}^{-1}$) and sources (nitrate and urea) for the analyzed phenological stages (V6, V10, PF, and FF), in the municipality of Nossa Senhora das Dores, state of Sergipe, Northeast Brazil.

| Actual evapotranspiration – ET (mm d ⁻¹) | | | | | | | |
|--|-----------------|------------------|--------------|--------------|--------------|--------------|--------------|
| N levels Date | PS ^a | 0Nt ^b | 50Nt | 100Nt | 150Nt | 200Nt | 250Nt |
| July 11 | V6 | 1.96 ± 1.23a | 1.97 ± 1.24a | 2.08 ± 1.28a | 1.98 ± 1.31a | 2.33 ± 1.30a | 2.12 ± 1.31a |
| July 21 | V10 | 2.88 ± 1.21a | 2.90 ± 1.20a | 3.06 ± 1.10a | 2.92 ± 1.15a | 2.88 ± 1.06a | 2.90 ± 1.05a |
| August 04 | PF | 4.26 ± 1.21a | 4.10 ± 1.48a | 4.12 ± 1.45a | 4.10 ± 1.37a | 4.07 ± 1.31a | 4.04 ± 1.32a |
| August 11 | FF | 4.54 ± 1.76a | 4.39 ± 1.58a | 4.35 ± 1.63a | 4.44 ± 1.57a | 4.37 ± 1.39a | 4.35 ± 1.51a |
| Mean | – | 3.41 ± 1.35a | 3.34 ± 1.38a | 3.40 ± 1.37a | 3.36 ± 1.35a | 3.41 ± 1.27a | 3.35 ± 1.30a |
| Actual evapotranspiration - ET (mm d ⁻¹) | | | | | | | |
| N levels Date | PS | 0Ur ^c | 50Ur | 100Ur | 150Ur | 200Ur | 250Ur |
| July 11 | V6 | 1.96 ± 1.23a | 2.19 ± 1.28a | 2.33 ± 1.30a | 2.27 ± 1.26a | 2.32 ± 1.32a | 2.30 ± 1.32a |
| July 21 | V10 | 2.88 ± 1.21a | 2.86 ± 1.19a | 3.00 ± 1.13a | 3.07 ± 1.13a | 3.08 ± 1.10a | 2.91 ± 1.00a |
| August 04 | PF | 4.26 ± 1.21a | 4.35 ± 1.51a | 4.29 ± 1.44a | 4.32 ± 1.33a | 4.27 ± 1.33a | 4.13 ± 1.38a |
| August 11 | FF | 4.54 ± 1.76a | 4.44 ± 1.61a | 4.41 ± 1.74a | 4.53 ± 1.58a | 4.51 ± 1.62a | 4.46 ± 1.36a |
| Mean | – | 3.41 ± 1.35a | 3.46 ± 1.40a | 3.51 ± 1.40a | 3.55 ± 1.33a | 3.55 ± 1.34a | 3.45 ± 1.27a |

^a PS: Phenological stages.

^b Nt: Nitrate.

^c Ur: Urea. V6 – Vegetative stage with six leaves per plant, V10 – Vegetative stage with ten leaves per plant, PF – Reproductive pre flowering, and FF – Reproductive full flowering. ET rates with the same letter in each line indicate no significant differences from each other at 5% (pairwise comparisons using the Tukey HSD post-hoc test performed by group with four repetitions for each PS).

conditions.

In the PF stage (August 04, DOY 216), the highest ET rates happened with N cover fertilizing at 50 kg ha^{-1} for Ur (50Ur) and 100 kg ha^{-1} for Nt (100Nt), but respectively only 2% and 3% higher than those for the control treatment (0NtUr). Considering all corn plots, the average ET

rates for Ur source were only 4% higher than those for Nt one. The previous 10-day P and ET_0 values were respectively of 55.0 and 34.0 mm, resulting in a climatic water excess of 21.0 mm. The ET_r values were above 0.98 for both N cover fertilizing sources, but averaging 1.00 and 1.04 for Nt and Ur, respectively.

Table 5

Two-way ANOVA considering interactions between 2 nitrogen (N) sources (nitrate – Nt and urea – Ur), 11 N levels (0–250 kg ha⁻¹), and 4 phenological stages – PS (vegetative with six leaves – V6, vegetative with ten leaves – V10, pre-flowering – PF, and Full Flowering – FF), for actual evapotranspiration – ET.

| Actual Evapotranspiration - ET (mm d ⁻¹) | | | | |
|--|-----|---------|--------|--------------|
| | df | F Value | Pr > F | Significance |
| N sources and levels | 1 | 2.271 | 0.134 | ns |
| Phenological Stages | 3 | 403.124 | <2e-16 | *** |
| Interaction | 3 | 1.028 | 0.382 | ns |
| Residuals | 168 | | | |

Note: Pr < 0.05 is statistically significant at 5 percent significant level; ns = not significant; * Pr ≤ 0.05, ** Pr ≤ 0.01, *** Pr ≤ 0.001.

During the FF stage (August 11, DOY 223), the highest ET rates were for the treatment with no N cover fertilizing (0NtUr) and for 150Ur. Regarding all corn plots, the average pixel values for Ur were only 2% higher than those for Nt. The previous 10-day P and ET₀ values were respectively of 12.0 and 36.0 mm, resulted in a climatic water deficit of 24.0 mm, which was not so strong to drop the ET rates, due to the still high root-zone moisture levels. The ET_r values were above 1.00 for both N cover fertilizing sources, but averaging 1.03 and 1.04 for Nt and Ur, respectively, again indicating good water storage in the root-zone from the previous rainier period at the highest soil cover conditions.

ET rates were affected by crop development but according to the Tukey's HSD post-hoc test, by the same letter in each line, there were no significant differences among N cover fertilizing levels and sources inside each specific PS. Their magnitudes were most affected by variations on root-zone moisture levels, which in turn depend on the weather conditions and the ET partitions into transpiration (T) and soil evaporation (E), making difficult to distinguish the effects of N treatments inside a PS, because of the alternated magnitudes of T and E according to soil

cover (Fandiño et al., 2012; Consoli and Vanella, 2014; Rosa et al., 2016; Longo-Minnolo et al., 2020).

The high ET SD values indicated variabilities in the root-zone moisture and soil cover conditions, which affected the ET partitions, as the pixel sizes are of only 4 cm in a large amount of 6000 pixels involving mixed drier and moistier conditions favoring T or soil E from corn canopies or bare soil, respectively. Teixeira et al. (2014a) applying the SAFER algorithm in rainfed corn crop from Central West Brazil with MODIS images, found annual ET SD value of 0.80 mm d⁻¹, 58% of our average one, because of the low-resolution images (250 m) not separating very well corn plants and bare soil as in case of the 4-cm resolution of the Sq images.

Under well corn root-zone moisture levels, the ET at potential rates (ET_p) can be obtained by selecting the pixel values under these conditions, and the crop coefficients (K_c) estimated as the ratio of ET_p to ET₀ (Teixeira et al., 2014b). Then, by doing this selection, and considering all N cover fertilizing treatments, K_c ranged from 0.75 to 1.35, inside the standard tabulated values reported by Allen et al. (1998) and the ones found by DeJonge et al. (2012) for corn crop. In North western China, modelling and field measurements in corn crop retrieved average daily ET of 3.5 mm d⁻¹ (Ding et al., 2013), close to our averaged value. These K_c and ET similar values among the current results and those from literature bring confidence for estimating ET from SAFER applications with aerial camera onboard a RPA.

3.3. Biomass production

Fig. 8 shows the spatial distribution, average pixel values, and standard deviations (SD), for the daily values of corn biomass production (BIO), considering the analyzed phenological stages (PS) during the year 2017.

As for ET, it is also clearly perceived spatial and temporal variations

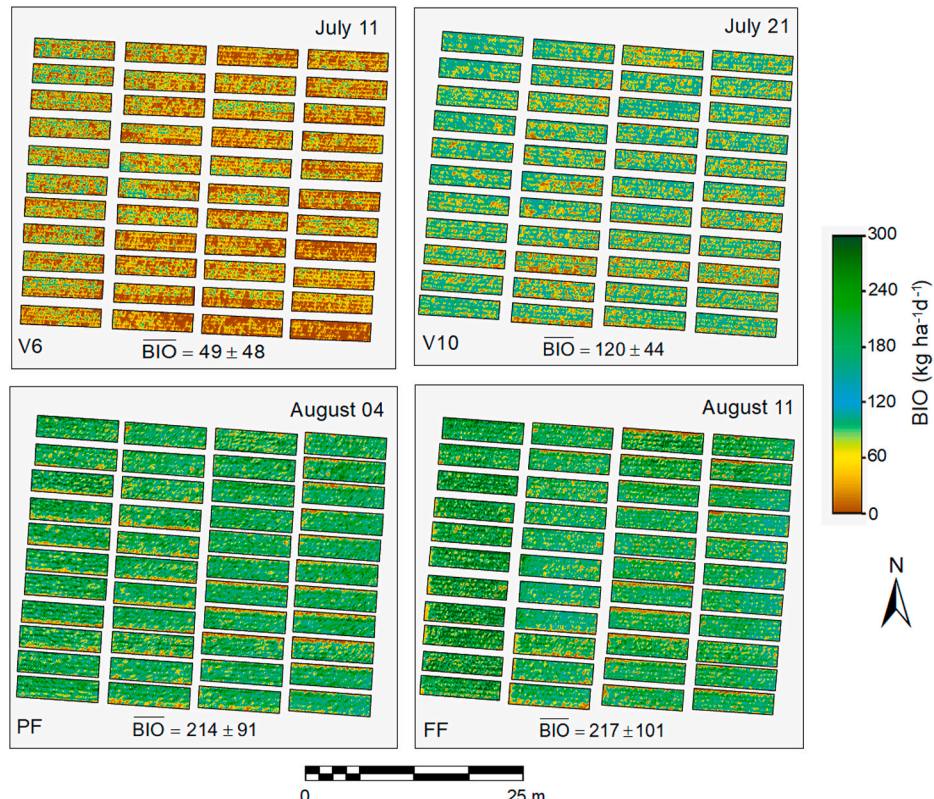


Fig. 8. Spatial distribution, average pixel values, and standard deviations (SD), for the daily pixel rates of corn biomass production (BIO), during four analyzed phenological stages (PS) in 2017. V6 – Vegetative stage with six leaves per plant (July 11, DOY 192), V10 – vegetative stage with ten leaves per plant (July 21, DOY 202), PF – reproductive stage pre flowering (August 04, DOY 216), and FF – reproductive full flowering (August 11, DOY 223).

on BIO pixel values in the images from Fig. 8, but in this case more noticeable the effects of canopy development, for all N cover fertilizing treatments. Comparing the representative images of the V6 and FF stages, BIO rates raised 4.4 folds. However, differently from ET, which rates are also influenced by soil evaporation at good soil moisture conditions, the spatial variations rapidly decreased as the canopies developed, with SD values dropping from 97% in V6 to 40% of the average BIO pixel values already in the V10 stage.

To assess BIO differences for each of the eleven N cover fertilizing treatments inside the analyzed PS, the 6000-pixel averages and SD values in the center of each corn plot were also considered. Besides corn BIO rates being related to the climatic water balance they also depend on solar radiation interception by plants for photosynthetic activities. Thus, to assess BIO we considered P, ET_r , and R_G ten-day period values prior the RPA flight dates.

Table 6 presents average BIO and SD values, according to the N cover fertilizing levels and sources with four repetitions for the rainfed corn crop, together with the results of the pairwise comparison by group, using the Tukey HSD post-hoc test performed for each PS, while **Table 7** shows detailed results of the ANOVA test for BIO.

In the V6 stage (July 11, DOY 192), the highest BIO values were for N cover fertilizing level of 100 kg ha⁻¹ for both Nt and Ur N sources, 130% of those for the ONtUr control treatment. However, from the Tukey HSD post-hoc test, there were no significant differences for N levels from 50 to 200 kg ha⁻¹. Considering the average values for this PS, BIO rates for Ur were only 2% higher than those for Nt. Although the 10-days previous climatic water excess of 36.0 mm. The low R_G values around 16.0 MJ m⁻² d⁻¹ and low canopy development for radiation interception reducing transpiration during this PS, were not in favor for high BIO rates.

During the V10 stage, the corn plots with N cover applications at 150 kg ha⁻¹ for both sources (150NtUr) presented the highest BIO rates, above respectively 28 and 23% of those for the N cover fertilizing control treatment (ONtUr). According to the Tukey HSD post-hoc test, the highest difference among treatments was for 150Nt. Averaging all plots, BIO values with Nt cover applications were only 1% higher than those with Ur. In this PS, according to the previous climatic conditions there was water deficit ($P - ET < 0$) of 11.0 mm, but the ET_r values above 0.98 for both N cover fertilizing sources indicated good root-zone moisture levels. However, the still low R_G average of 18 MJ m⁻² d⁻¹ limited somewhat the BIO rates, even at increasing soil cover conditions.

Table 6

Average pixel values and standard deviations (SD) for biomass production (BIO), considering the N cover fertilizing levels (0–250 kg ha⁻¹) and sources (nitrate and urea) for the analyzed phenological stages (V6, V10, PF, and FF), in the municipality of Nossa Senhora das Dores, state of Sergipe, Northeast Brazil.

| N levels Dates | Biomass production – BIO (kg ha ⁻¹ d ⁻¹) | | | | | | | |
|---|---|------------------|------------|------------|------------|------------|-----------|-----------|
| | PS ^a | 0Nt ^b | 50Nt | 100Nt | 150Nt | 200Nt | 250Nt | Mean |
| July 07 | V6 | 40 ± 41a | 51 ± 45c | 52 ± 47c | 50 ± 49c | 50 ± 52c | 44 ± 49b | 48 ± 47 |
| July 21 | V10 | 105 ± 64a | 118 ± 67b | 115 ± 65b | 134 ± 66c | 120 ± 61b | 121 ± 61b | 119 ± 64 |
| August 04 | PF | 192 ± 22a | 230 ± 102c | 221 ± 100b | 222 ± 94b | 215 ± 92b | 217 ± 93b | 216 ± 100 |
| August 11 | FF | 200 ± 111a | 244 ± 101c | 206 ± 105b | 215 ± 101b | 228 ± 88b | 222 ± 96b | 219 ± 100 |
| Mean | – | 134 ± 60a | 161 ± 79c | 149 ± 79b | 155 ± 78b | 153 ± 73b | 151 ± 75b | 151 ± 78 |
| Biomass production – BIO (kg ha ⁻¹ d ⁻¹) | | | | | | | | |
| N levels Dates | PS | 0Ur ^c | 50Ur | 100Ur | 150Ur | 200Ur | 250Ur | Mean |
| July 07 | V6 | 40 ± 41a | 50 ± 46b | 51 ± 49b | 50 ± 46b | 51 ± 49b | 50 ± 51b | 49 ± 47 |
| July 21 | V10 | 105 ± 64a | 117 ± 67b | 117 ± 65b | 129 ± 66b | 121 ± 63b | 121 ± 58b | 118 ± 64 |
| August 04 | PF | 192 ± 22a | 210 ± 103b | 210 ± 98b | 218 ± 92c | 209 ± 92b | 211 ± 95c | 208 ± 100 |
| August 11 | FF | 200 ± 111a | 224 ± 103c | 205 ± 110b | 215 ± 102b | 211 ± 102b | 215 ± 87c | 212 ± 103 |
| Mean | – | 134 ± 60a | 150 ± 80b | 146 ± 81b | 153 ± 77b | 148 ± 77b | 149 ± 73c | 147 ± 79 |

^a PS: Phenological stage.

^b Nt: Nitrate.

^c Ur: Urea. V6 – Vegetative stage with six leaves per plant, V10 – Vegetative stage with ten leaves per plant, PF – Reproductive stage pre flowering, and FF – Reproductive stage full flowering. BIO rates with the same letter in each line are not significantly different from each other at 5% (pairwise comparisons using the Tukey HSD post-hoc test performed by group with four repetitions for each PS).

Table 7

Two-way ANOVA considering interactions between 2 nitrogen (N) sources (nitrate – Nt and urea – Ur), 11 N levels (0–250 kg ha⁻¹), and 4 phenological stages – PS (vegetative with six leaves – V6, vegetative with ten leaves – V10, pre-flowering – PF, and Full Flowering – FF), for biomass production – BIO.

| Biomass Production - BIO (kg ha ⁻¹ d ⁻¹) | | | | |
|---|-----|---------|---------|--------------|
| | df | F Value | Pr > F | Significance |
| N sources and levels | 1 | 10.206 | 0.00167 | ** |
| Phenological Stage | 3 | 886.542 | <2e-16 | *** |
| Interaction | 3 | 0.146 | 0.93219 | ns |
| Residuals | 168 | | | |

Note: Pr < 0.05 is statistically significant at 5 percent significant level; ns = not significant; * Pr ≤ 0.05, ** Pr ≤ 0.01, *** Pr ≤ 0.001.

In the PF stage, the highest BIO values for Nt source happened already with N cover fertilizing at 50 kg ha⁻¹ (50Nt), while for Ur, this was at 250 kg ha⁻¹ (250Ur), above respectively 20 and 10% of the ONtUr control treatment, the largest differences according to the Tukey HSD post-hoc test. Considering all N cover fertilizing levels, the average BIO rate for Nt was 4% above of that for Ur. The previous water excess in the 10-day climatic water balance of 21.0 mm, maintained the ET_r values above 1.02 for both N cover fertilizing sources, with R_G averaging 19.0 MJ m⁻² d⁻¹. The conditions of increasing solar radiation interception by the canopies and high root-zone moisture levels promoted high BIO pixel values, above 200 kg ha d⁻¹ for all non-zero N cover fertilizing levels.

During the FF stage, the highest BIO rates were for both 50Nt and 50Ur treatments, above respectively 22% and 12% of the ONtUr control one, with both treatments presenting the highest statistical differences, according to the Tukey HSD post-hoc test. In average, the Nt source promoted BIO rates 3% higher than those for Ur. The previous 10-day P and ET_r values promoted a climatic water deficit of 24.0 mm, but the good root-zone moisture levels, with ET_r values around 1.04 for both N cover fertilizing sources, together with a continuously increase on solar radiation interception as consequence of crop development, with R_G averaging 20.0 MJ m⁻² d⁻¹, increased the BIO values to the highest level among the analyzed crop stages.

The FF stage presenting the maximum BIO values agrees with Taghvaeian et al. (2012) and Zhang et al. (2019), who found maximum values by using remote sensing vegetation indices in corn crop when the canopies were fully covering the soil. On the other hand, the R_G

increases in August in the current study increased the photosynthetic activity, which together crop development favoring transpiration brought BIO to maximum values (Yang et al., 2019). According to Kang et al. (2002) and Driscoll et al. (2006), transpiration promote high levels of photosynthetic activities, increasing BIO, under good root-zone moisture levels, what agrees with our results.

From Tables 4 and 6, it is noticed that N cover fertilizing did not significantly affect the ET rates, while BIO followed the development of leaf areas with increases on transpiration rates, being ET much related with its partition into transpiration and soil evaporation (Longo-Minnolo et al., 2020), which in turn are dependent on soil cover and PS stage (Rosa et al., 2016). Campos et al. (2018) and Twohey et al. (2019), by using remote sensing measurements, confirm high correlations between BIO and transpiration in both irrigated and rainfed corn crop, as the soil evaporation does not contribute to BIO.

As in case of ET, Teixeira et al. (2014a) applying the SAFER algorithm in rainfed corn crop from Central West Brazil with MODIS images, found annual BIO SD value of $39 \text{ kg ha}^{-1} \text{ d}^{-1}$, 50% of our average one, because of the 250-m low-resolution images causing pixel contaminations, which are reduced in case of our 4-cm resolution images. For ET and BIO, the soil moisture is considered through ET_r (Eq. (8)), but for BIO, the introduction of f_p (Eq. (12)), related to radiation interception by canopies, accounts for the effect of plant transpiration. Thus, the dynamic effects of the N cover fertilizing levels on water and vegetation conditions by using the remote sensing parameters should be better understood throughout the WP_{BIO} index along the corn crop stages.

3.4. Water productivity assessments

Under water scarcity scenarios, it is desirable good corn yield levels but under low water consumption, in such way that should not have no significant reductions on BIO at ET bellow ET_p . This is the importance of WP assessments under different N cover fertilizing levels. Regarding the corn PS, we analyzed the WP dynamics in terms of BIO (WP_{BIO}), while with the availability of actual yield (Y_a) data and up scaling ET and BIO remote-sensing parameters, we could also evaluate WP for the growing season (GS) based on Y_a (WP_{Y_a}) for each N cover fertilizing treatment.

3.4.1. Dynamics on water productivity

Taking into account the ratio of BIO to ET for the 6000 pixels in the

Table 8

Average pixel values and standard deviations (SD) of water productivity based on biomass production (WP_{BIO}), considering the N cover fertilizing levels (0–250 kg ha^{-1}) and sources (nitrate and urea), for the analyzed phenological stages (V6, V10, PF, and FF), in the municipality of Nossa Senhora das Dores, state of Sergipe, Northeast Brazil.

| N levels Dates | Water Productivity based on biomass production – WP_{BIO} (kg m^{-3}) | | | | | | | |
|---|---|-------------------------|-------------------------|-------------------------|-------------------------|-------------------------|-------------------------|-----------------|
| | PS ^a | 0Nt ^b | 50Nt | 100Nt | 150Nt | 200Nt | 250Nt | Mean |
| July 07 | V6 | $2.04 \pm 0.34\text{a}$ | $2.59 \pm 0.40\text{b}$ | $2.50 \pm 0.44\text{b}$ | $2.53 \pm 0.42\text{b}$ | $2.15 \pm 0.53\text{a}$ | $2.08 \pm 0.45\text{a}$ | 2.31 ± 0.43 |
| July 21 | V10 | $3.65 \pm 0.42\text{a}$ | $4.07 \pm 0.51\text{b}$ | $3.76 \pm 0.55\text{a}$ | $4.59 \pm 0.53\text{b}$ | $4.17 \pm 0.52\text{b}$ | $4.17 \pm 0.52\text{b}$ | 4.07 ± 0.51 |
| August 04 | PF | $4.51 \pm 0.47\text{a}$ | $5.61 \pm 0.51\text{b}$ | $5.36 \pm 0.52\text{b}$ | $5.41 \pm 0.52\text{b}$ | $5.28 \pm 0.52\text{b}$ | $5.37 \pm 0.52\text{b}$ | 5.26 ± 0.51 |
| August 11 | FF | $4.41 \pm 0.46\text{a}$ | $5.56 \pm 0.49\text{b}$ | $4.74 \pm 0.49\text{a}$ | $4.84 \pm 0.50\text{a}$ | $5.22 \pm 0.50\text{b}$ | $5.10 \pm 0.49\text{b}$ | 4.98 ± 0.49 |
| Mean | – | $3.94 \pm 0.42\text{a}$ | $4.46 \pm 0.48\text{b}$ | $4.09 \pm 0.50\text{a}$ | $4.34 \pm 0.49\text{b}$ | $4.20 \pm 0.52\text{b}$ | $4.18 \pm 0.50\text{b}$ | 4.15 ± 0.49 |
| Water Productivity based on biomass production – WP_{BIO} (kg m^{-3}) | | | | | | | | |
| N levels Date | PS | 0Ur ^c | 50Ur | 100Ur | 150Ur | 200Ur | 250Ur | |
| July 07 | V6 | $2.04 \pm 0.34\text{a}$ | $2.28 \pm 0.42\text{a}$ | $2.19 \pm 0.46\text{a}$ | $2.20 \pm 0.45\text{a}$ | $2.20 \pm 0.43\text{b}$ | $2.17 \pm 0.51\text{b}$ | 2.18 ± 0.43 |
| July 21 | V10 | $3.65 \pm 0.42\text{a}$ | $4.09 \pm 0.47\text{b}$ | $3.90 \pm 0.49\text{b}$ | $4.20 \pm 0.53\text{b}$ | $3.93 \pm 0.49\text{b}$ | $4.16 \pm 0.53\text{b}$ | 3.99 ± 0.49 |
| August 04 | PF | $4.51 \pm 0.47\text{a}$ | $4.83 \pm 0.51\text{b}$ | $4.90 \pm 0.52\text{b}$ | $5.05 \pm 0.54\text{b}$ | $4.89 \pm 0.51\text{b}$ | $5.11 \pm 0.54\text{b}$ | 4.88 ± 0.51 |
| August 11 | FF | $4.41 \pm 0.46\text{a}$ | $5.05 \pm 0.52\text{b}$ | $4.65 \pm 0.48\text{b}$ | $4.75 \pm 0.50\text{b}$ | $4.68 \pm 0.49\text{b}$ | $4.82 \pm 0.52\text{b}$ | 4.72 ± 0.49 |
| Mean | – | $3.94 \pm 0.42\text{a}$ | $4.06 \pm 0.48\text{a}$ | $3.91 \pm 0.49\text{b}$ | $4.05 \pm 0.51\text{b}$ | $3.92 \pm 0.48\text{b}$ | $4.07 \pm 0.53\text{b}$ | 3.94 ± 0.48 |

^a PS: Phenological stage.

^b Nt: Nitrate.

^c Ur: Urea. V6 – Vegetative stage with six leaves per plant, V10 – Vegetative stage with ten leaves per plant, PF – Reproductive stage pre flowering, and FF – Reproductive stage full flowering. WP_{BIO} values with the same letter in each line are not significantly different from each other at 5% (pairwise comparisons using the Tukey HSD post-hoc test performed for group with four repetitions for each PS).

center of each corn plots (see Fig. 1), for the eleven N cover fertilizing treatments with averages of four repetitions, we carried out the WP_{BIO} assessments considering the four analyzed PS.

Table 8 presents WP_{BIO} average and SD values, considering the N cover fertilizing levels and sources with four repetitions in the rainfed corn crop, together with the results of the pairwise comparison by group, using the Tukey HSD post-hoc test performed for each PS, while Table 9 presents detailed results of the ANOVA test for WP_{BIO} .

In the V6 stage, the highest WP_{BIO} values were for N cover fertilizing treatments of 50 kg ha^{-1} for both N sources, Nt and Ur, respectively above 27% and 12% above the control ones (ONtUr). The reasons for these highest values were the lowest ET rates, as BIO ones were high (see also Tables 4 and 6). N cover fertilizing with Nt retrieved WP_{BIO} values 6% higher than those for Ur, because the higher ET rates for Ur source. The BIO values for Ur did not differ from those the control (ONtUr), according to Tukey HSD post-hoc test. Due to low R_G levels affecting BIO together with the lowest soil cover by canopies for radiation interception, WP_{BIO} in this PS presented the lowest values comparing with the other stages.

During the V10 stage, the plots N cover fertilizing at 150 kg ha^{-1} presented the highest WP_{BIO} rates for both Nt and Ur source, above respectively for 26% and 15% of the ONtUr control treatment, with significant statistical differences according to the Tukey HSD test. The main reason was the highest BIO values, as for ET there were no

Table 9

Two-way ANOVA considering interactions between 2 nitrogen (N) sources (nitrate – Nt and urea – Ur), 11 N levels (0–250 kg ha^{-1}), and 4 phenological stages – PS (vegetative with six leaves – V6, vegetative with ten leaves – V10, pre-flowering – PF, and Full Flowering – FF), for water productivity based on biomass production – WP_{BIO} .

Water productivity based on BIO – WP_{BIO} (kg m^{-3})

| | df | F Value | Pr > F | Significance |
|----------------------|-----|---------|----------|--------------|
| N sources and levels | 1 | 52.20 | 1.67e-11 | *** |
| Phenological Stage | 3 | 2181.42 | <2e-16 | *** |
| Interaction | 3 | 1.02 | 0.385 | ns |
| Residuals | 168 | | | |

Note: $Pr < 0.05$ is statistically significant at 5 percent significant level; ns = not significant; * $Pr \leq 0.05$, ** $Pr \leq 0.01$, *** $Pr \leq 0.001$.

significant differences among treatments. Considering all corn plots, WP_{BIO} values for Nt source were only 2% higher than those for Ur. Still low both R_G levels restricted somewhat the BIO values and then WP_{BIO} in this PS, even with increasing soil cover by canopies for radiation interception.

In the PF stage, the highest WP_{BIO} pixel values were for the 50Nt and 250Ur treatments, respectively 24 and 13% higher than the control N treatment (0NtUr), presenting statistical differences according to the Tukey HSD test. The main reason was high BIO rates, highlighting those for the Nt source. Considering the averages for all corn plots, Nt source promoted WP_{BIO} values 8% higher than those for Ur, mainly due the lower Nt ET rates. This PS was characterized as the one of the highest WP_{BIO} , because of the coupled effect of the previous climatic water excess maintaining high ET_r values, together with R_G and soil cover increases for radiation interception, favoring the BIO rates.

In the FF stage, the highest WP_{BIO} values were for N cover fertilizing level at 50 kg ha⁻¹ for both Nt and Ur N sources, above 25 and 15% of the control treatment (0NtUr). The highest values were again for Nt applications (6% higher than those for Ur). The climatic water deficit did not drop ET to affect WP_{BIO} values below those of the previous PS, as their BIO rates were not significantly different under high both ET_r values and radiation interception levels.

According to the WP_{BIO} values from Table 8, there were variations among N cover fertilizing treatments due to root-zone moisture, crop development, and R_G values. These variations together with soil stains and germination failures made sometimes difficult to understand the effects of N cover fertilizing treatments on ET and BIO pixel variations, and then on WP_{BIO} , inside a PS. However, considering the four

repetitions for each N cover fertilizing treatments, it is clearly noticed from the statistical analyses, that the N cover at 150 kg ha⁻¹ for both, Nt and Ur sources, should be the best option for having good corn yields while promoting water saving, avoiding N leaching to the ground water.

3.4.2. Growing season water productivity

Having actual yield (Y_a) data available (weight of grains) for each N cover fertilizing treatment, besides WP_{BIO} , it was also possible to carried out WP_{Y_a} assessments for the whole growing season (GS), up scaling the ratio of ET to $ET_0 - ET_r$ (Eq. (8)) and the fraction of the photosynthetically active radiation that is absorbed by the corn canopy – f_p (Eqs. (12) and (15)).

We considered $ET_r = 0.30$ for the Sowing (S) stage and $ET_r = 0.50$ for the harvest (H) stage following Allen et al. (1998) and Teixeira et al. (2014b). From the Full Flowering (FF) to Harvest (H) stages we took an average to infer a representative value from the Grain Filling (GF) to Physiological Maturation (PM) transition stages (see also Table 2). The suitability of using interpolated vegetation indices to follow crop stages has been demonstrated by Mateos et al. (2013). Thus, curves were built relating six ET_r values with DD_{ac} for each N cover fertilizing treatment (Fig. 9):

The assumption of the same ET_r values for the S and H stages for all N cover fertilizing treatments is plausible, as in the S stage there was no corn plants and in the H stage, they were under senescence conditions. Low ET_r values indicate the degree of water stress (Lu et al., 2011), and as the curves depicted in Fig. 9 shows values bellow the standard corn K_c values (Venancio et al., 2021), it is clear some degree of root-zone moisture stress along the corn GS, which should have affected

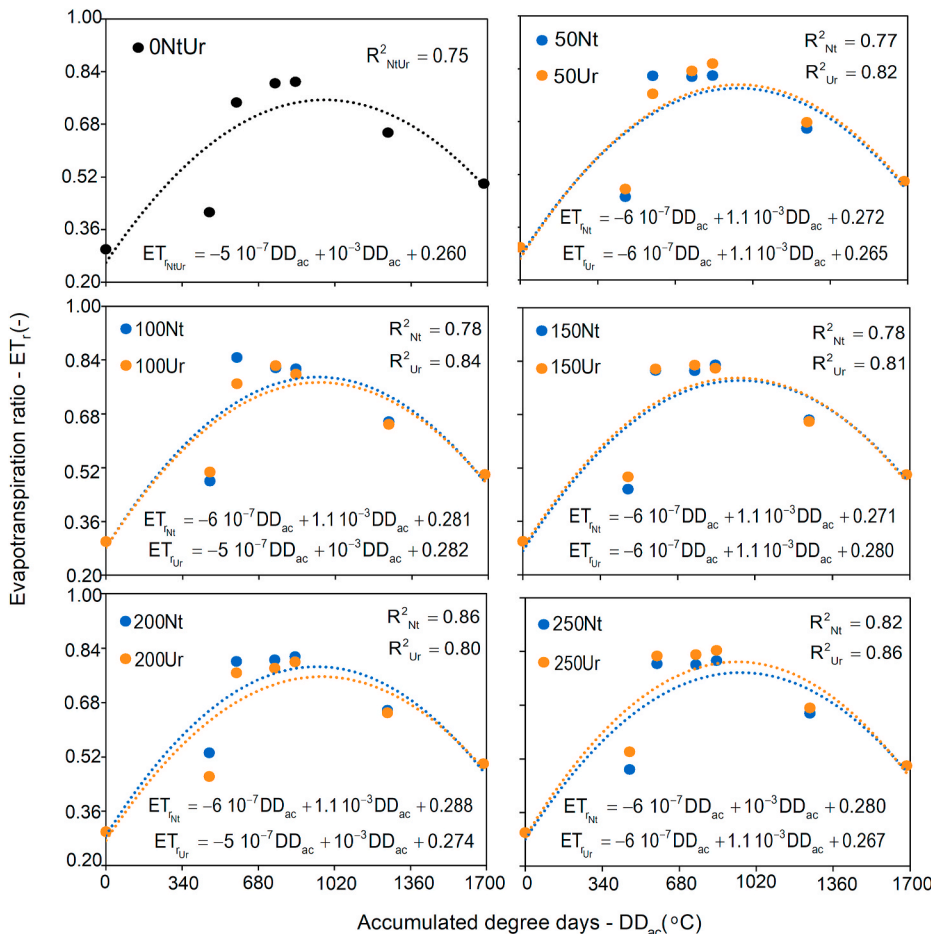


Fig. 9. Relationships between the ratio of actual (ET) to reference (ET_0) evapotranspiration values ($ET_r = ET/ET_0$), and the corn accumulated degree-days (DD_{ac}), considering different nitrogen (N) cover fertilizing treatments. N levels of 0, 50, 100, 150, 200, and 250 kg ha⁻¹, through nitrate (Nt) and urea (Ur) N sources.

somewhat WP_{Y_a} (Trout et al., 2017; Wang et al., 2017; Liao et al., 2019).

The resulted ET_r values from the equations represented by the curves from Fig. 9 were multiplied by ET_0 calculated by using the weather data close to the experimental area resulting into GS ET rates for each N cover fertilizing treatment. After estimating the average ET_r values, Eq. (15) was used to estimate the GS f_p values. Thus, with the GS values of f_p , ET_r , ET_0 , R_G , and Y_a , corn WP_{BIO} and WP_{Y_a} at the GS timescale were assessed applying Eq. (14).

Fig. 10 shows the GS values of ET, BIO, and Y_a , considering all N cover fertilizing levels and sources for the studied rainfed corn crop.

The highest GS ET value was for the 250Ur treatment (394.6 mm GS^{-1}), but only 0.4 mm GS^{-1} above of that for the control (0NtUr) (Fig. 10a). The highest GS Y_a and BIO values were for the N cover fertilizing level of 150 kg ha^{-1} for both N sources (averages of 9.8 and 17.7 t $ha^{-1} GS^{-1}$, respectively), but not significantly different from those for 200 and 250 kg ha^{-1} (only 1–2% above). The mean GS values for Y_a and BIO were 8.77 and 8.74 t $ha^{-1} GS^{-1}$, and 17.32 and 17.28 t $ha^{-1} GS^{-1}$, respectively for Nt and Ur N sources.

Considering the harvest index (HI) as the ratio of Y_a to BIO, it ranged from 0.37 to 0.55 for the respective treatments without N cover fertilizing (0NtUr) and those for N cover applications at 150 kg ha^{-1} for both N sources, averaging 0.50 and 0.51, for Nt and Ur, respectively. This HI range agrees with, who found values from 0.20 to 0.56 for corn under different growing conditions in South Romania. Nyolei et al. (2019) reported average corn ET, Y_a and BIO respective values of 331.0 mm, 3.2 t ha^{-1} , and 6.8 t ha^{-1} , yielding an average HI of 0.47, coupling Sentinel and Landsat 8 images in the north-eastern part of Tanzania. However, this last study involved different corn growth stages and pixel contaminations with other crops.

As we did not have ET and BIO field measurements, to validate the modelling equations, the similarity of HI values between our study and those from literature bring confidence for the WP results, as we had availability of accurate Y_a data from mechanical harvester machine. These similarities and accurate grain yield measurements, together with calibration of the modelling equations taking Landsat measurements as reference, compensated somewhat the lack of advance field energy and water balance measurements, allowed reliable WP comparisons among different N cover fertilizing treatments for the studied rainfed corn crop.

The GS WP_{BIO} and WP_{Y_a} average values for nitrate (subscript Nt) and urea (subscript Ur) N sources are presented in Table 10:

The highest BIO and Y_a values together with low ET rates for Nt source favored slightly higher WP values when comparing with those for Ur source. The top WP values were for N cover applications at 150 kg ha^{-1} , however stabilizing after this level for both N sources.

The average WP_{Y_a} from Table 10 is higher than that found by Nyolei et al. (2019) of 0.97 kg m^{-3} in Tanzania, but these last authors attributed their lower values to low yields obtained in the mid and lowlands areas of their study region. However, Teixeira et al. (2014a), using MODIS images, reported an average value of 2.1 kg m^{-3} for rainfed corn crop in

Table 10

Average pixel values for the water productivity based on biomass production – BIO (WP_{BIO}) and based on actual yield – Y_a (WP_{Y_a}), considering cover fertilizing with different nitrogen (N) levels and sources for the rainfed corn growing season (GS), in the municipality of Nossa Senhora das Dores, state of Sergipe, Northeast Brazil.

| Water Productivity based on biomass production – $WP_{BIO}(kg m^{-3})$ | | | | | | | |
|--|------|------|------|------|------|------|------|
| N levels N sources | 0 | 50 | 100 | 150 | 200 | 250 | Mean |
| Nitrate – Nt | 4.14 | 4.39 | 4.43 | 4.51 | 4.47 | 4.48 | 4.40 |
| Urea – Ur | 4.14 | 4.36 | 4.40 | 4.48 | 4.45 | 4.46 | 4.38 |
| Mean | 4.14 | 4.38 | 4.42 | 4.50 | 4.46 | 4.47 | 4.39 |
| Water Productivity based on actual yield – $WP_{Y_a}(kg m^{-3})$ | | | | | | | |
| N levels N sources | 0 | 50 | 100 | 150 | 200 | 250 | Mean |
| Nitrate – Nt | 1.55 | 2.18 | 2.25 | 2.49 | 2.43 | 2.45 | 2.23 |
| Urea – Ur | 1.55 | 2.16 | 2.24 | 2.48 | 2.41 | 2.43 | 2.21 |
| Mean | 1.55 | 2.17 | 2.25 | 2.49 | 2.42 | 2.44 | 2.22 |

the state of Mato Grosso, Central West Brazil, while for pivot irrigated corn, Teixeira et al. (2014b) using Landsat 8 images found WP_{Y_a} average of 2.0 kg m^{-3} in the state of São Paulo, Southeast Brazil.

The stabilization at N cover fertilizing at 150 kg ha^{-1} , means that farmers applying N above this level will lose money and increase the risk of more N leaching to the ground water. Considering the WP_{Y_a} values and the corn grain prices in 2017, the monetary counterparts was around U \$0.50 m^{-3} for both N sources with the recommended N cover fertilizing level at 150 kg ha^{-1} . However, the advantage of the price of kg of Ur being 63% of that for Nt is summed with its lower N leaching rates, promoting less environmental problems.

Corn rainfed WP monetary values in the current study are inside of those for irrigated corn in Southeast Brazil (0.34–0.68 US\$ m^{-3}) (Teixeira et al., 2014b) and for irrigated dwarf coconut in Northeast Brazil (0.23–0.58 US\$ m^{-3}) (Teixeira et al., 2019), but higher than those for other arable crops around the world (0.10–0.20 US\$ m^{-3}) (Sakthivadivel et al., 1999), and much lower than for table grapes (3.4–8.8 US\$ m^{-3} , respectively) and mangos (2.2–5.1 US\$ m^{-3}) in Northeast Brazil (Teixeira et al., 2009). However, besides these differences, other issues are important to consider in the rainfed corn WP assessments, as for example, the overall production costs and environmental impacts.

4. Conclusions

The joint applications of the SAFER algorithm and the Monteith' RUE model with radiation measurements in the ranges of visible and near infra-red bands of images from a camera onboard a remotely piloted aircraft (RPA) together with weather and yield data, allowed the rainfed

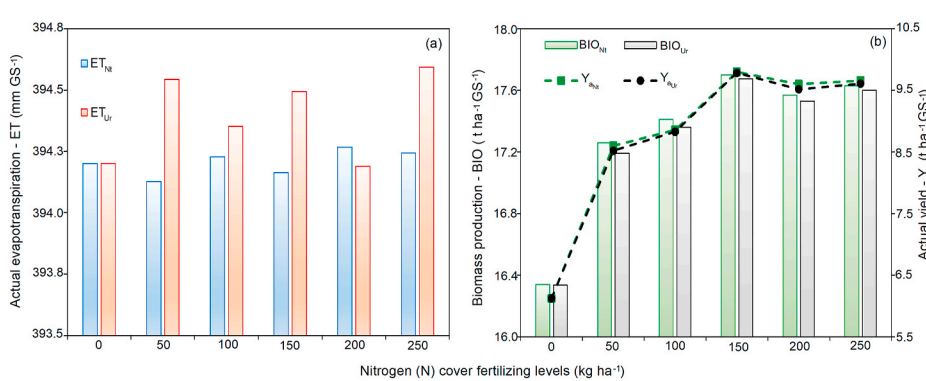


Fig. 10. Growing season (GS) values for the water productivity (WP) components. Actual evapotranspiration – ET (a); biomass production – BIO and actual yield – Y_a (b), for nitrogen (N) cover fertilizing levels (0–250 kg ha^{-1}) and sources from nitrate (subscript Nt) and urea (subscript Ur).

corn water productivity assessments at high spatial resolution (4 cm), with detections of the effect of N cover fertilizing under different levels and sources in Northeast Brazil.

Although differences on actual evapotranspiration (ET) levels were not significant among nitrogen (N) cover applications ranging from 0 to 250 kg ha⁻¹, due proportional variations in ET partition into soil evaporation and canopy transpiration along the phenological stages, differences on biomass production (BIO), promoted different water productivity (WP) values, stabilizing at N cover fertilizing levels of 150 kg ha⁻¹ for both nitrate (Nt) and urea (Ur) N sources. This means that with N cover fertilizing levels above this N level will promote money losses and increase risks of negative environmental effects of N leaching rates to the ground water.

Considering the slightly lower WP values for Ur N cover fertilizing applications comparing with those for Nt ones, and the advantage of the lower price and less leaching problems for Ur, this N source at 150 kg ha⁻¹ is recommended to avoid environmental problems, while saving money.

The successfully applications of the models with the reference crop and region encourage the replication of the methods with aerial cameras onboard a remotely piloted aircrafts (RPA) in other WP studies, being probably necessary only calibrations and validations of the modelling equations for specific environmental conditions.

Author contributions

Antônio H. de C. Teixeira – The first author was responsible for running the models to acquire the water productivity components, conceptualizations, writing the manuscript, for visualization of figures, analyses' results, software resources, for supervision, project administration, and funding acquisition.

Edson P. Pacheco – The second author oversaw the ARP flights, constructing image mosaics, formatting of weather data for reference evapotranspiration calculations, and the methodology, data curation, and investigation.

Cesar de O. F. Silva – Collaborated with image processing, oversaw running scripts, software running, visualization of the figures, methodology, data curation, and editing the manuscript.

Marcia G. Dompieri – Review, validation, and editing of the manuscript, and analyses' results. Janice F. Leivas – Review, validation, and editing of the manuscript, and analyses' results.

Funding

This research was funded by Brazilian National Research Council (in Portuguese: *Conselho Nacional de Desenvolvimento Científico e Tecnológico - CNPq*), grant numbers 404229/2013-1 and 446136/2015-8.

Ethical statement

The authors declare that all ethical practices have been followed in relation to the development, writing and publication of the work reported in this paper.

Declaration of competing interest

The authors declare that they have no known competing financial interests or personal relationships that could have appeared to influence the work reported in this paper.

Acknowledgments

To the National Council for Scientific and Technological Development (CNPQ), for the financial support to our projects on energy and water balances.

References

- Allen, R.G., Pereira, L.S., Raes, D., Smith, M., 1998. Crop Evapotranspiration: Guidelines for Computing Crop Water Requirements. FAO Irrigation and Drainage Paper 56, Rome, Italy, 300pp.
- Allen, R.G., Tasumi, M., Morse, A., Trezza, R., Wright, J.L., Bastiaanssen, W.G.M., Kramber, W., Lorite, I., Robison, C.W., 2007. Satellite-based energy balance for mapping evapotranspiration with internalized calibration (METRIC) - Applications. *J. Irrigat. Drain. Eng.* 133, 395–406.
- Araujo, L.M., Teixeira, A.H. de C., Bassoi, L.H., 2019. Evapotranspiration and biomass modelling in the Pontal Sul irrigation scheme. *Int. J. Rem. Sens.* 1, 1–13.
- Bakhsh, A., Jaynes, D.B., Colvin, T.S., Kanwar, R.S., 2000. Spatio-temporal analysis of yield variability for a corn-soybean field in Iowa. *Trans. ASAE (Am. Soc. Agric. Eng.)* 43 (1), 31–38.
- Ballabio, C., Panagos, P., Monatanarella, L., 2016. Mapping topsoil physical properties at European scale using the LUCAS database. *Geoderma* 261, 110–123.
- Ballabio, C., Lugato, E., Fernández-Ugalde, O., Orgiazzi, A., Jones, A., Borrelli, P., Montanarella, L., Panagos, P., 2019. Mapping LUCAS topsoil chemical properties at European scale using Gaussian process regression. *Geoderma* 355, 113912.
- Bastiaanssen, W.G.M., Ali, S., 2003. A new crop yield forecasting model based on satellite measurements applied across the Indus Basin, Pakistan. *Agric. Ecosyst. Environ.* 94, 321–340.
- Campos, I., Neale, C.M.U., Arkebauer, T.J., Suyker, A.E., Gonçalves, I.Z., 2018. Water productivity and crop yield: a simplified remote sensing driven operational approach. *Agric. Meteorol.* 249, 501–511.
- Castelli, M., Asam, S., Jacob, A., Zebisch, M., Notarnicola, C., 2018. Monitoring daily evapotranspiration in the Alps exploiting Sentinel-2 and meteorological data. In: Proceedings of the Remote Sensing and Hydrology Symposium (ICRS-IAHS), Cordoba, Spain, May 8-10, 2018.
- Colaço, A.F., Bramley, R.G.V., 2018. Do crop sensors promote improved nitrogen management in grain crops? *Field Crop. Res.* 218, 126–140.
- Consoli, S., Vanella, D., 2014. Comparisons of satellite-based models for estimating evapotranspiration fluxes. *J. Hydrol.* 513, 475–489.
- Dehziari, S.A., Sanaieejad, S.H., 2019. Energy balance quantification using Landsat 8 images and SAFER algorithm in Mashhad, Razavi Khorasan, Iran. *J. Appl. Remote Sens.* 13, 014528.
- Dejonge, K.C., Ascough, J.C., Andales, A.A., Handen, N.C., Garcia, L.A., Arabi, M., 2012. Improving evapotranspiration simulations in the CERES-Maize model under limited irrigation. *Agric. Water Manag.* 115, 92–113.
- Ding, R., Kang, S., Li, F., Zhang, Y., Tong, L., 2013. Evapotranspiration measurement and estimation using modified Priestly-Taylor model in irrigated maize field with mulching. *Agric. For. Meteorol.* 168, 140–148, 2013.
- Driscoll, S.P., Prins, A., Olmos, E., Kunert, K.J., Foyer, C.H., 2006. Specification of adaxial and abaxial stomata, epidermal structure and photosynthesis to CO₂ enrichment in maize leaves. *J. Exp. Bot.* 57, 381–390.
- Fancelli, A.L., Dourado Neto, D., 2000. Ecophysiology and Fenología. In: Fancelli, A.L., Dourado Neto, D. (Eds.), Produção de Milho. Guapiaçuá, pp. 21–54.
- Fandino, M., Cancela, J.J., Rey, B.J., Martínez, E.M., Rosa, R.G., Pereira, L.S., 2012. Using the dual-Kc approach to model evapotranspiration of Albariño vineyards (*Vitis vinifera* L. cv. Albariño) with consideration of active ground cover. *Agric. Water Manag.* 112, 75–87.
- Gago, J., Doutre, C., Coopman, R.E., Gallego, P.P., Ribas-Carbo, M., Flexas, J., Escalona, J., Medrano, H., 2015. UAVchallenge to assess water stress for sustainable agriculture. *Agric. Water Manag.* 153, 9–19.
- Kang, S., Zhang, F., Hu, X., Zhang, J., 2002. Benefits of CO₂ enrichment on crop plants are modified by soil water status. *Plant Soil* 238, 69–77.
- Ko, J., Piccini, G., 2009. Corn yield responses under crop evapotranspiration-based irrigation management. *Agric. Water Manag.* 96, 799–808.
- Leivas, J.F., Teixeira, A.H. de C., Silva, G.B., Garçon, E.A.M., Ronquim, C.C., 2017. Water indicators based on SPOT 6 satellite images in irrigated area at the Paracatu River Basin, Brazil. *Proc. SPIE* 10421, 1042111-1–1042111-7.
- Liao, C., Wang, J., Dong, T., Shang, J., Liu, J., Song, Y., 2019. Using spatio-temporal fusion of Landsat-8 and MODIS data to derive phenology, biomass and yield estimates for corn and soybean. *Sci. Total Environ.* 650, 1707–1721.
- Liu, J., Pattey, E., Miller, J.R., McNairn, H., Smith, A., Hu, B., 2010. Estimating crop stresses, aboveground dry biomass and yield of corn using multi-temporal optical data combined with a radiation use efficiency model. *Remote Sens. Environ.* 114, 1167–1177.
- Longo-Minnolo, G., Vanella, D., Consoli, S., Intrigliolo, D.S., Ramirez-Cuesta, J.M., 2020. Integrating forecast meteorological data into the ArcDualKc model for estimating spatially distributed evapotranspiration rates of a citrus orchard. *Agric. Water Manag.* 231, 105967.
- Lu, N., Chen, S., Wilske, B., Sun, G., Chen, J., 2011. Evapotranspiration and soil water relationships in a range of disturbed and undisturbed ecosystems in the semi-arid Inner Mongolia, China. *J. Plant Ecol.* 4, 49–60.
- Maes, W.H., Steppé, K., 2019. Perspectives for remote sensing with unmanned aerial vehicles in precision agriculture. *Trends Plant Sci.* 24, 152–164.
- Mahlein, A.-K., Oerke, E.-C., Steiner, U., Dehne, H.-W., 2012. Recent advances in sensing plant diseases for precision crop protection. *Eur. J. Plant Pathol.* 133 (1), 197–209.
- Manfreda, S., McCabe, M.F., Miller, P.E., Lucas, R., Madrigal, V.P., Mallinis, G., Dor, E.B., Helman, D., Estes, L., Ciraolo, G., et al., 2018. On the use of unmanned aerial systems for environmental monitoring. *Rem. Sens.* 10, 641.
- Marino, S., Cocozza, C., Tognetti, R., Alvino, A., 2015. Use of proximal sensing and vegetation indexes to detect the inefficient spatial allocation of drip irrigation in a spot area of tomato field crop. *Precis. Agric.* 16, 613–629.

- Mateos, L., González-Dugo, M.P., Testi, L., Villalobos, F.J., 2013. Monitoring evapotranspiration of irrigated crops using crop coefficients derived from time series of satellite images. I. Method validation. *Agric. Water Manag.* 125, 81–91.
- McShane, R.R., Driscoll, P.K., Sando, R., 2017. A Review of Surface Energy Balance Models for Estimating Actual Evapotranspiration with Remote Sensing at High Spatiotemporal Resolution over Large Extents. *Scientific Investigations Report 2017-5087*. U.S. Geological Survey, Reston, VA, USA, 19pp.
- Mokhtari, A., Noory, H., Pourshakouri, F., Haghightamehr, P., Afrasiabian, Y., Razavi, M., Fereydooni, F., Naeni, A.S., 2019. Calculating potential evapotranspiration and single crop coefficient based on energy balance equation using Landsat 8 and Sentinel-2. *ISPRS J. Photogrammetry Remote Sens.* 154, 231–245.
- Monteith, J.L., 1977. Climate and efficiency of crop production in Britain. *Philos. T. R. So. B* 281, 277–294.
- Mulla, D.J., 2013. Twenty-five years of remote sensing in precision agriculture: key advances and remaining knowledge gaps. *Biosyst. Eng.* 114, 358–371.
- Nagler, P.L., Glenn, E.P., Nguyen, U., Scott, R.L., Doody, T., 2013. Estimating riparian and agricultural actual evapotranspiration by reference evapotranspiration and MODIS enhanced vegetation index. *Rem. Sens.* 5, 3849–3871.
- Nyolei, D., Nsaali, M., Minaya, V., van Grienven, A., Mbilinyi, B., Diels, J., Hessels, T., Kahimba, F., 2019. High resolution mapping of agricultural water productivity using SEBAL in a cultivated African catchment, Tanzania. *Phys. Chem. Earth* 112, 36–39.
- Pacheco, E.P., Dompieri, M.H.G., Teixeira, A.H. de C., Couto, J.P. de A., Hayashi, C.H., 2018. Estudo preliminar para recomendação de adubação nitrogenada na cultura do milho em função do NDVI calculado a partir de imagens aéreas. Anais do Congresso Brasileiro de Agricultura de Precisão. Curitiba, Paraná, 2018.
- Pádua, L., Vanko, J., Hruška, J., Adão, T., Sousa, J.J., Peres, E., Morais, R., 2017. UAS, sensors, and data processing in agroforestry: a review towards practical applications. *Int. J. Rem. Sens.* 38, 2349–2391.
- Ramírez-Cuesta, J.M., Vanella, D., Consoli, S., Motisi, A., Minacapilli, M., 2018. A satellite stand-alone procedure for deriving net radiation by using SEVIRI and MODIS products. *Int. J. Appl. Earth Obs. Geoinformation* 73, 786–799.
- Rampazo, N.A.M., Picoli, M.C.A., Teixeira, A.H. de C., Cavaliero, C.K.N., 2020. Water consumption modeling by coupling MODIS images and agrometeorological data for sugarcane crops. *Sugar Tech.* <https://doi.org/10.1007/s12355-020-00919-7>.
- Rosa, R.D., Ramos, T.B., Pereira, L.S., 2016. The dual Kc approach to assess maize and sweet sorghum transpiration and soil evaporation under saline conditions: application of the SIMDualKc model. *Agric. Water Manag.* 177, 77–94.
- Rozenstein, O., Haymann, N., Kaplan, G., Tanny, J., 2018. Estimating cotton water consumption using a time series of Sentinel-2 imagery. *Agric. Water Manag.* 207, 44–52.
- Sakthivadivel, R., de Fraiture, C., Molden, D.J., Perry, C., Kloezeman, W., 1999. Indicators of land and water productivity irrigated agriculture. *Int. J. Water Resour. Dev.* 15, 161–180.
- Santos, J.E.O., Cunha, F.F., Filgueiras, R., Silva, G.H., Teixeira, A.H. de C., Silva, F.C.S., Sediyyama, G.C., 2020. Performance of SAFER evapotranspiration using missing meteorological data. *Agric. Water Manag.* 233, 1–8.
- Sedina, J., Pavelka, K., Raeva, P., 2017. UAV remote sensing capability for precision agriculture, forestry, and small natural reservation monitoring. *Proc. SPIE* 10213, 102130L-1–102130L-12, 2017.
- Senay, G.B., Schauer, M., Friedrichs, M., Velpuri, N.M., Ramesh, K.S., 2017. Satellite based water use dynamics using historical Landsat data (1984–2014) in the southwestern United States. *Remote Sens. Environ.* 202, 98–112.
- Sharma, L., Bali, S., 2018. A review of methods to improve nitrogen use efficiency in agriculture. *Sustainability* 10 (51), 1–23.
- Silva, C.O.F., Teixeira, A.H. de C., Manzione, R.L., 2019. Agriwater: an R package for spatial modelling of energy balance and actual evapotranspiration using satellite images and agrometeorological data. *Environ. Model. Software* 120, 1–19.
- Taghvaeian, S., Chávez, J.L., Hansen, N.C., 2012. Infrared thermometry to estimate crop water stress index and water use of irrigated maize in northeastern Colorado. *Rem. Sens.* 4, 3619–3637.
- Teixeira, A.H. de C., Bastiaanssen, W.G.M., Ahmad, M.-ud-D., Bos, M.G., 2009. Reviewing SEBAL input parameters for assessing evapotranspiration and water productivity for the Low-Middle São Francisco River basin, Brazil Part B: application to the large scale. *Agric. For. Meteorol.* 149, 477–490.
- Teixeira, A.H. de C., 2010. Determining regional actual evapotranspiration of irrigated and natural vegetation in the São Francisco river basin (Brazil) using remote sensing and Penman-Monteith equation. *Rem. Sens.* 2, 1287–1319.
- Teixeira, A.H. de C., Victoria, D. de C., Andrade, R.G., Leivas, J.F., Bolfe, E.L., Cruz, C.R., 2014a. Coupling MODIS images and agrometeorological data for agricultural water productivity analyses in the Mato Grosso state, Brazil. *Proc. SPIE* 9239, 92390W-1–92390W-14, 2014a.
- Teixeira, A.H. de C., Hernandez, F.B.T., Andrade, R.G., Leivas, J.F., Victoria, D. de C., Bolfe, E.L., 2014b. Irrigation performance assessments for corn crop with Landsat images in the São Paulo state, Brazil. *Water Res. Irrig. Manage.* 3, 91–100.
- Teixeira, A.H. de C., Takemura, C.M., Leivas, J.F., Pacheco, E.P., Bayma-Silva, G., Garçon, E.A.M., 2019. Water productivity assessments for dwarf coconut by using Landsat 8 images and agrometeorological data. *ISPRS J. Photogrammetry Remote Sens.* 155, 150–158.
- Teixeira, A.H. de C., Takemura, C.M., Leivas, J.F., Pacheco, E.P., Bayma-Silva, G., Garçon, E.A.M., 2020a. Water productivity monitoring by using geotechnological tools in contrasting social and environmental conditions: applications in the São Francisco River basin, Brazil. *Remote Sens. Appl.: Soc. Environ.* 18, 100296.
- Teixeira, A.H. de C., Leivas, J.F., Garçon, E.A.M., Takemura, C.M., Quartaroli, C.F., Alvarez, I.A., 2020b. Modeling large-scale biometeorological indices to monitor agricultural-growing areas: applications in the fruit circuit region, São Paulo, Brazil. *Int. J. Biometeorol.* <https://doi.org/10.1007/s00484-020-01996-9>.
- Togeiro de Alckmin, G., Kooistra, L., Rawnsley, R., et al., 2020. Comparing methods to estimate perennial ryegrass biomass: canopy height and spectral vegetation indices. *Precis. Agric.* <https://doi.org/10.1007/s11119-020-09737-z>.
- Trout, T.J., DeJonge, K.C., 2017. Water productivity of maize in the US high plains. *Irrigat. Sci.* 35, 251–266.
- Tunca, E., Köksal, E.S., Çetin, S., Ekiz, N.M., Balde, H., 2018. Yield and leaf area index estimations for sunflower plants using unmanned aerial vehicle images. *Environ. Monit. Assess.* 190, 682.
- Twohey, R.J., Roberts, L.M., Studer, A.J., 2019. Leaf stable carbon isotope composition reflects transpiration efficiency in Zea mays. *Plant J.* 97, 475–484.
- Vanino, S., Nino, P., Micheleb, C.D., Bolognesi, S.F., D'Urso, G., Bene, C.D., Pennelli, B., Vuolo, F., Farina, R., Pulighe, G., Napoli, R., 2018. Capability of Sentinel-2 data for estimating maximum evapotranspiration and irrigation requirements for tomato crop in Central Italy. *Remote Sens. Environ.* 215, 452–470.
- Venancio, L.P., Mantovani, E.C., do, Amaral C.H., Neale, C.M.U., Filgueiras, R., Ivo Zution Gonçalves, I.Z., Cunha, F.F. da, 2021. Evapotranspiration mapping of commercial corn fields in Brazil using SAFER algorithm. *Sci. Agric.* 78, 1–12.
- Wang, Y., Janz, B., Engedad, T., De Neergaard, A., 2017. Effect of irrigation regimes and nitrogen rates on water use efficiency and nitrogen uptake in maize. *Agric. Water Manag.* 179, 271–276.
- Yang, Y., Xu, W., Hou, P., Liu, G., Liu, W., Wang, Y., Zhao, R., Ming, B., Xie, R., Wang, K., et al., 2019. Improving maize grain yield by matching maize growth and solar radiation. *Sci. Rep.* 9, 1–11.
- Yigini, Y., Panagos, P., 2016. Assessment of soil organic carbon stocks under future climate and land cover changes in Europe. *Sci. Total Environ.* 557, 838–850.
- Zhang, L., Niu, Y., Zhang, H., Han, W., Li, G., Tang, J., Peng, X., 2019. Maize canopy temperature extracted from UAV thermal and RGB imagery and its application in water stress monitoring. *Front. Plant Sci.* 10, 1–18.